

# Design and In-Silico Evaluation of Pyridine-4-Carbohydrazide Derivatives for Potential Therapeutic Applications

Sofian S. Mohamed <sup>1</sup>, Salah M Bensaber <sup>2</sup>, Nisreen H Meiqal <sup>2</sup>, Anton Hermann <sup>3</sup>, Abdul M Gbaj <sup>2\*</sup>

<sup>1</sup>Department of Chemistry and Toxins, Judicial Expertise and Research Center, Tripoli, Libya.

<sup>2</sup>Department of Medicinal Chemistry, Faculty of Pharmacy, University of Tripoli, Tripoli, Libya.

<sup>3</sup>Department of Biosciences, University of Salzburg, Salzburg, Austria.

**\*Corresponding Author:** Abdul M Gbaj, Professor of Genetics and Biochemistry, Department of Medicinal Chemistry, Faculty of Pharmacy, University of Tripoli, Tripoli, Libya.

**Received Date:** February 10, 2025; **Accepted Date:** February 26, 2025; **Published Date:** March 05, 2025

**Citation:** Sofian S. Mohamed, Salah M. Bensaber, Nisreen H. Meiqal, Anton Hermann, Abdul M. Gbaj, (2025), Design and In-Silico Evaluation of Pyridine-4-Carbohydrazide Derivatives for Potential Therapeutic Applications, *J. Surgical Case Reports and Images*, 8(3); DOI:10.31579/2690-1897/235

**Copyright:** © 2025, Abdul M Gbaj. This is an open access article distributed under the Creative Commons Attribution License, which permits unrestricted use, distribution, and reproduction in any medium, provided the original work is properly cited.

## Abstract

The emergence of drug-resistant and novel diseases underscores the urgency for innovative therapeutic interventions. Drug repositioning and computational approaches offer an efficient pathway to accelerate drug discovery and development. This study leverages these techniques in designing and evaluating derivatives based on the FDA-approved compound, pyridine-4-carbohydrazide, to assess how structural modifications impact therapeutic potential.

**Methods:** The derivatives were designed using a chemical library of small molecules containing imine functional groups, built upon pyridine-4-carbohydrazide scaffolds (INH01-INH19). Computational tools, including Molinspiration Cheminformatics, way2drug, and the pkCSM platform, were utilized to evaluate each derivative's physicochemical properties, drug-likeness, bioactivity scores, potential biological activities, and ADME (Absorption, Distribution, Metabolism, Excretion) profiles.

**Results:** Most derivatives demonstrated enhanced physicochemical characteristics, adhering to both Lipinski's Rule of Five and Veber's Rule. Bioactivity scores varied with moderate to inactive interactions across six target classes, ranked as follows: enzyme inhibitors, kinase inhibitors, G-protein-coupled receptors, protease inhibitors, nuclear receptors, and ion channel modulators. Notably, derivatives INH03, INH09, INH14, and INH19 exhibited high predicted activity in multiple therapeutic areas, indicating potential applications in antibacterial, antiviral, antiprotozoal, anti-inflammatory and anticancer treatments. Moreover, structural modifications in these derivatives positively influenced ADME profiles compared to pyridine-4-carbohydrazide, though certain compounds presented challenges, such as limited solubility, P-glycoprotein interactions and CYP450 inhibition.

**Conclusions:** These Schiff base derivatives stand out as promising candidates for further drug development, underscoring the importance of computational strategies in optimizing drug discovery and design.

**Keywords:** drug discovery; drug repositioning; in-silico study; adme properties

## Introduction

A drug, in the context of medicine, is a chemical or biological substance designed to interact with biological processes within an organism to treat, diagnose, or prevent disease (Benedetti, 2014). These agents can originate from diverse sources, including natural, semisynthetic, or synthetic origins (Pollock et al., 2024). The continuous need for new medications arises from several factors, including the toxicity and side effects of existing drugs (Kroschinsky et al., 2017), the emergence of new

diseases (Khan et al., 2020), the development of drug resistance (Jackson et al., 2018), and advancements in our understanding of health conditions (Subbiah, 2023). These challenges actuate pharmaceutical research and development to innovate, improve treatment efficacy and address previously unmet medical needs. The traditional process of drug discovery follows a well-established procedure, beginning with the identification and validation of molecular targets (Salazar & Gormley,

2017). This is typically followed by high-throughput screening of extensive chemical libraries to identify potential lead compounds (Sinha & Vohora, 2017). Conventional drug discovery methods heavily rely on empirical approaches, involving extensive *in vitro* and *in vivo* testing to evaluate a compound's efficacy, pharmacokinetics and toxicity. Although this approach has led to the development of numerous successful therapies, it is both time-consuming and costly, often requiring over a decade and more than \$2.5 billion to successfully bring a new drug to market (Kumari et al., 2022; Schlander et al., 2021). To overcome these challenges, alternative approaches such as drug repurposing, also known as drug repositioning, have gained prominence (Ahmad et al., 2021; Talevi & Bellera, 2020a). Drug repositioning involves identifying new therapeutic uses for existing drugs, whether FDA-approved, withdrawn, or outdated. This approach leverages the well-established safety profiles of known drugs, allowing for faster and less costly drug development (Gazerani, 2019). Drug repositioning can also involve using an existing drug as a template for synthesizing new analogs that exhibit activity against other diseases (Cha et al., 2018). This strategy has distinct advantages over conventional drug discovery, including shorter development timelines, reduced investment needs, and higher success rates (Pushpakom et al., 2018; Wu et al., 2019). Approximately 33% of drugs approved in recent years have resulted from drug repositioning efforts, underscoring its effectiveness as a modern drug discovery strategy (Talevi & Bellera, 2020b).

Advances in computational technologies, bioinformatics, and proteomics have significantly accelerated the drug discovery process through the integration of *in-silico* methods (Liao et al., 2022). Computational approaches, commonly known as computer-aided drug design (CADD), have become indispensable tools at every stage of drug development (Kapetanovic, 2008). CADD enables the transformation of biological target information into computational models, allowing for data computation, analysis, and the prediction of compound activities. Molecular docking, virtual screening, and machine learning help filter large chemical libraries into smaller, more promising subsets for experimental validation. Moreover, CADD offers critical insights for lead compound optimization, focusing on improving binding affinity, pharmacokinetics, and toxicity profiles, as well as designing novel compounds via structural modifications (Sliwoski et al., 2014). The benefits of CADD are vast, providing substantial reductions in the time, cost, and experimental scope traditionally required for drug discovery. By predicting and optimizing compound properties *in silico*, CADD can shorten the research timeline and reduce development costs by up to 50% (Sachin S Padole et al., 2022; Xiang et al., 2012). Additionally, as computational accuracy continues to improve, these predictions increasingly align with experimental outcomes, bolstering the credibility and reliability of *in silico* approaches. Today, CADD is widely employed in the search for treatments for a range of diseases, including cancer (Chua et al., 2023; Reddy et al., 2007), Diabetes (Balamurugan et al., 2012; Semighini et al., 2011), and infectious diseases caused by viruses (Chen et al., 1994; Doyon et al., 2005; Yang et al., 2024) and bacteria (Duan et al., 2019; Njogu et al., 2016; Supuran, 2017).

Pyridine-4-carbohydrazide, commonly known as isoniazid, has served as a cornerstone in the treatment of tuberculosis. Its efficacy stems from its ability to inhibit the synthesis of mycolic acids, essential components of the mycobacterial cell wall (Vilchèze & Jacobs, 2019). The chemical structure of isoniazid, as depicted in Figure 1, presents a versatile

molecular framework for the development of agents with a broad spectrum of biological activities. One of the common approaches is replacing the hydrazide hydrogen with different functional groups can alter the molecule's polarity, hydrophobicity, hydrogen bonding capacity, and overall molecular conformation (Mali et al., 2021; Raczuk et al., 2022). This versatility has led to the synthesis of a plethora of derivatives with expanded therapeutic applications such as anti-inflammatory (Zhang et al., 2020), antitubercular (Aboui-Fadl et al., 2003), anticancer (Firmino et al., 2016; Rodrigues et al., 2014), antimicrobial and urease inhibitory activity (Habala et al., 2016), antidepressant and analgesic properties (Uddin et al., 2020), in the treatment of Alzheimer's disease (Santos et al., 2020). Additionally, the pyridine moiety itself plays a crucial role in enhancing drug permeability, biochemical potency, and metabolic stability. Moreover, the pyridine ring's ability to form various non-covalent interactions with protein targets facilitates drug-target binding (Ling et al., 2021; Pennington & Moustakas, 2017). The FDA database provides compelling evidence of the prevalence of pyridine-based drugs. Approximately 18% of approved heterocyclic drugs incorporate pyridine or its derivatives, highlighting its significance as a structural motif in medicinal chemistry (Ling et al., 2021).

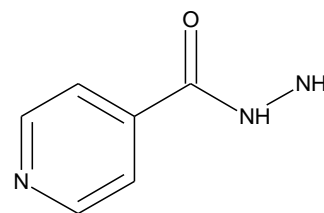


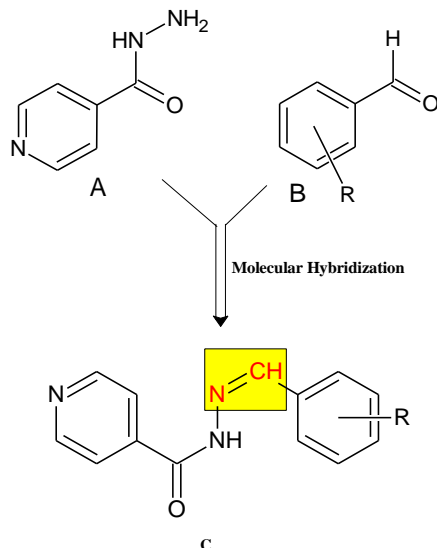
**Figure 1:** Chemical structure of Pyridine-4-Carbohydrazide (Isoniazid, INH).

Based on these advancements, this study aims to design and evaluate a chemical library of small molecules incorporating imine functional groups and pyridine-4-carbohydrazide scaffolds. Leveraging computational methods, we will predict the physicochemical properties, drug-likeness, bioactivity profiles, and ADME characteristics of these derivatives before synthesis and screening. By doing so, we aim to reduce resource waste and avoid unnecessary time and expenses associated with screening compounds that have a low likelihood of activity. This screening approach is intended to streamline the identification of promising agents, enhancing the efficiency of the drug discovery pipeline and reducing the risk of failure in later stages.

## Materials and Methods

### Design Strategy

In this study, compounds (Schiff bases) were designed by utilizing the FDA-approved drug pyridine-4-carbohydrazide (A) and hybridized with substituted aldehydes (B). The imine group (C), formed during this process, was used to augment the lipophilic behavior part, as illustrated in Scheme 1. The R groups vary in type, position, partition coefficient, and hydrogen bonding capacity. This modification was intended to investigate the influence of various substituents on the phenyl ring and their impact on the biological activity of these compounds. A total of nineteen compounds were designed and assigned the code INH01-INH19.



**Scheme 1:** The Design Concept for Schiff Base Compounds

(probably use large letter C in the figure!)

### *In silico* Study

This study was conducted using a HP computer system with the following specifications: Windows 11 operating system, Intel® Core™ i5-1135G7 Quad-core Processor @ 2.40GHz, and 8 Gigabytes of RAM. The chemical structures of nineteen compounds (INH01-INH19) were initially generated using the ChemDraw software suite as in Table 1A. The *in-silico* workflow commenced with the preparation of molecular structures for the designed compounds. These structures were first constructed in the two-dimensional (2D) format using Chem3D Ultra software and saved in the Structure Data File (SDF) format. The 2D molecular representations were then converted into SMILES (Simplified Molecular Input Line Entry System) format using the online SMILES Translator tool provided by the National Cancer Institute (<https://cactus.nci.nih.gov/translate/>). To ensure structural accuracy, the resulting SMILES strings were meticulously validated against their original chemical structures, as detailed in Table 1B. Following validation, the SMILES data served as the key input for subsequent predictive analysis. The data was uploaded to various online platforms, enabling the calculation of essential molecular properties and the prediction of potential biological activities for the designed compounds. This computational workflow provided valuable insights into the physicochemical, drug-likeness, bioactivity, and pharmacokinetic characteristics of the pyridine-4-carbohydrazide derivatives under

investigation. The specific online platforms employed and the details of the obtained predictions are elaborated upon in subsequent sections.

### Physicochemical, Drug-likeness, and bioactivity Properties predictions

The physicochemical properties, drug-likeness, and bioactivity of the compounds were evaluated using the molinspirationchemoinformatics platform. Drug-likeness assessments were conducted according to Lipinski's Rule of Five and Veber's rules. Additionally, the platform predicted bioactivity against six different protein targets: GPCR, ICM, KI, NRC, PI, and EI.

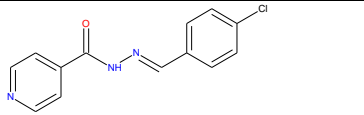
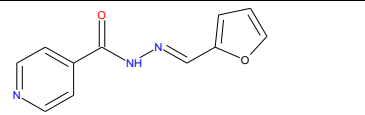
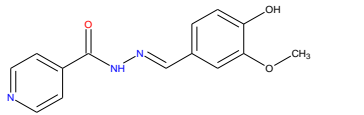
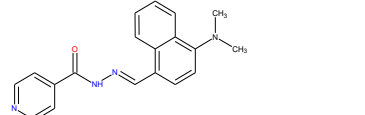
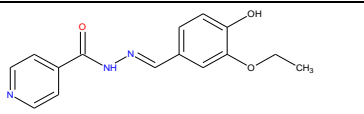
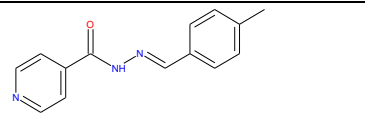
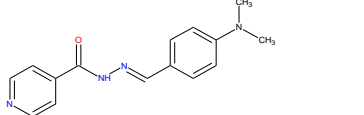
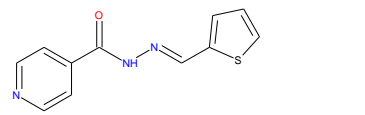
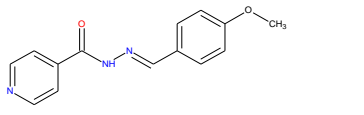
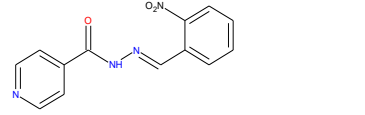
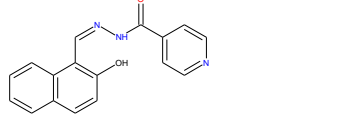
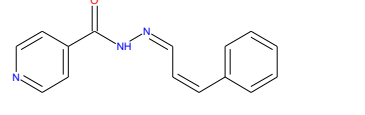
### Prediction of Activity Spectra for Substances (PASS)

To further elucidate the biological activity spectrum of the pyridine-4-carbohydrazide derivatives, the PASS online tool (<https://www.way2drug.com/passonline/>) was employed.

### ADME Prediction

The ADME properties of the derivatives were predicted using the pkCSM-Pharmacokinetics software (<https://biosig.lab.uq.edu.au/pkcsm/>). Established methodologies documented in the scientific literature served as the foundation for these predictions.

Codes	Chemical Structure	Codes	Chemical Structure
INH01		INH10	
INH02		INH11	
INH03		INH12	

<b>INH04</b>		<b>INH13</b>	
<b>INH05</b>		<b>INH14</b>	
<b>INH06</b>		<b>INH15</b>	
<b>INH07</b>		<b>INH16</b>	
<b>INH08</b>		<b>INH17</b>	
<b>INH09</b>		<b>INH18</b>	
<b>INH19</b>			

**Table 1A:** Codes and chemical Structures of the designed compounds.

Codes	Character	
<b>NH01</b>	IUPAC name	N'-[phenylmethylidene] pyridine-4-carbohydrazide
	SMILES	<chem>O=C(NN=Cc1ccccc1)c2ccncc2</chem>
<b>NH02</b>	IUPAC name	N-(2-hydroxybenzylidene) pyridine-4-carbohydrazide
	SMILES	<chem>O=C(NN=Cc1ccccc1O)c2ccncc2</chem>
<b>NH03</b>	IUPAC name	N'-[(3-nitrophenyl) methylidene] pyridine-4-carbohydrazide
	SMILES	<chem>C1=CC(=CC(=C1)[N+](=O)[O-])C=NNC(=O)C2=CC=NC=C2</chem>
<b>NH04</b>	IUPAC name	N'-[(Z)-(4-Chlorophenyl) methylidene] pyridine-4-carbohydrazide
	SMILES	<chem>C1C=CC=C(\C=N\NC(=O)C2=CC=NC=C2)C=C1</chem>
<b>NH05</b>	IUPAC name	N-[(4-Hydroxy-3-methoxybenzylidene) pyridine-4-carbohydrazide
	SMILES	<chem>COC1=C(C=CC(=C1)C=NNC(=O)C2=CC=NC=C2)O</chem>
<b>NH06</b>	IUPAC name	(N'-(3-ethoxy-4-hydroxybenzylidene) pyridine-4-carbohydrazide
	SMILES	<chem>CCOc2cc(C=NNC(=O)c1ccccc1)ccc2O</chem>
<b>NH07</b>	IUPAC name	N-(4-(dimethylamino) benzylidene) pyridine-4-carbohydrazide
	SMILES	<chem>CN(C)C1=CC=C(C=C1)C=NNC(=O)C2=CC=NC=C2</chem>
<b>NH08</b>	IUPAC name	(E)-N'-(4-methoxybenzylidene) pyridine-4-carbohydrazide
	SMILES	<chem>COc2ccc(C=NNC(=O)c1ccccc1)cc2</chem>
<b>NH09</b>	IUPAC name	(E)-N'-((2-hydroxynaphthalen-1-yl) methylene) pyridine-4-carbohydrazide
	SMILES	<chem>O=C(NN=Cc1c(O)ccc2ccccc12)c3ccncc3</chem>
<b>NH10</b>	IUPAC name	N'-(2-methoxy-4-nitrobenzylidene) pyridine-4-carbohydrazide
	SMILES	<chem>COc1cc(N(=O)=O)ccc1C=NNC(=O)c2ccncc2</chem>
<b>NH11</b>	IUPAC name	N'-(2-hydroxy-5-methoxybenzylidene) pyridine-4-carbohydrazide

	SMILES	<chem>COc2ccc(O)c(C=NNC(=O)c1ccncc1)c2</chem>
NH12	IUPAC name	N <sup>1</sup> -(4-nitrobenzylidene) pyridine-4-carbohydrazide
	SMILES	<chem>O=C(NN=Cc1ccc(N(=O)=O)cc1)c2ccncc2</chem>
NH13	IUPAC name	N <sup>1</sup> -(furan-2-ylmethylene)pyridine-4-carbohydrazide
	SMILES	<chem>O=C(NN=Cc1ccco1)c2ccncc2</chem>
NH14	IUPAC name	N <sup>1</sup> -((4-(dimethylamino) naphthalen-1-yl) methylene) pyridine-4-carbohydrazide
	SMILES	<chem>CN(C)c2ccc(C=NNC(=O)c1ccncc1)c3cccc23</chem>
NH15	IUPAC name	N-(4-methylbenzylidene) pyridine-4-carbohydrazide
	SMILES	<chem>CC1=CC=C(C=C1)C=NNC(=O)C2=CC=NC=C2</chem>
NH16	IUPAC name	N <sup>1</sup> -[thiophen-2-yl] pyridine-4-carbohydrazide
	SMILES	<chem>C1=CSC(=C1)/C=N\NC(=O)C2=CC=NC=C2</chem>
NH17	IUPAC name	N <sup>1</sup> -[(2-nitrophenyl) methylidene] pyridine-4-carbohydrazide
	SMILES	<chem>C1=CC=C(C(=C1)/C=N\NC(=O)C2=CC=NC=C2)[N+](=O)[O-]</chem>
NH18	IUPAC name	N-[(E)-[(Z)-3-phenylprop-2-enylidene]amino] pyridine-4-carbohydrazide
	SMILES	<chem>C1=CC=C(C=C1)/C=C\C=N\NC(=O)C2=CC=NC=C2</chem>
NH19	IUPAC name	N <sup>1</sup> -[(E)-(naphthalen-2-yl) methylidene] pyridine-4-carbohydrazide
	SMILES	<chem>O=C(NN=Cc1cccc2cccc12)c3ccncc3</chem>
NH	IUPAC name	Pyridine-4-carbohydrazide
	SMILES	<chem>C1=CN=CC=C1C(=O)NN</chem>

Table 1B: IUPAC names and canonical SMILES of the predicted compounds.

Parameter	Predictor	Unit	Requirement value
<b>Physiochemical and drug-likeness properties</b>			
Lipinski's Rule	Molecular weight (MW)	g/mol	<500
	Partition coefficient (LogP)	-	< 5
	Number of hydrogen bond acceptors	-	<10
	Number of hydrogen bond donors	-	< 5
Veber Rule	Number of rotatable bonds (N-rotb)	-	< 5
	Topological polar surface area (TPSA)	-	<140
<b>Bioactivity score properties</b>			
Bioactivity score	G-protein-coupledreceptor ligands (GPCR)	-	▪ Compounds with a bioactivity score greater than 0.00 are considered active.
	Ion channel modulation (ICM)	-	
	Kinase inhibitor (KI)	-	
	Nuclear receptor ligands (NRL)	-	▪ Compounds with a bioactivity score ranging from -0.50 to 0.00 are moderately active.
	Protease inhibitor (PI)	-	▪ Compounds with a bioactivity score less than -0.50 are deemed inactive.
	Enzyme inhibitor (EI)	-	
<b>Pharmacokinetic properties</b>			
Absorption	Water solubility	LogS	-
	Intestinal absorption (HIA)	% Absorbed	▪ High absorption: %Abs > 30% ▪ Poorly absorption: %Abs < 30%
	Caco-2 permeability (Caco-2)	log Papp in 10 <sup>-6</sup> cm/s	High permeability > 0.90

Parameter	Predictor	Unit	Requirement value
	Skin permeability (SP)	log Kp	Logkp> -2.5
	P-glycoprotein substrate (P-gp)	Yes / No	-
	P-glycoprotein I inhibitor	Yes / No	-
	P-glycoprotein II inhibitor	Yes / No	-
Distribution	The volume of distribution (VD <sub>ss</sub> )	log L/kg	Low: VD <sub>ss</sub> < -0.15 and high: VD <sub>ss</sub> > 0.45
	Fraction unbound (FU)	-	High > 0.45
	BBB permeability (BBB)	log BB	<ul style="list-style-type: none"> <li>▪ LogBB Value &lt; -1: poorly.</li> <li>▪ LogBB Value &gt; 0.3: crosses the BBB.</li> </ul>
	CNS permeability	log PS	<ul style="list-style-type: none"> <li>▪ Log PS Value &lt; -3: unable to penetrate.</li> <li>▪ Log PS Value &gt; -2: penetrates CNS.</li> </ul>
Metabolism	CYP1A2 inhibitor	Yes / No	-
	CYP3A4 substrate/inhibitor	Yes / No	-
	CYP2C8 inhibitor	Yes / No	-
	CYP2C9 substrate/inhibitor	Yes / No	-
	CYP2C19 inhibitor	Yes / No	-
	CYP2D6 substrate/inhibitor	Yes / No	-
Excretion	Total clearance (CL <sub>tot</sub> )	log mL/min/kg	Higher is better
	Renal OCT2 substrate	Yes / No	-

**Table 1C:** Distribution of predictors used in the *in-Silico* Study.

## Results and discussion

### Design strategy

This study presents an approach to the repositioning of isoniazid by introducing structural modifications at the terminal at the terminal NH<sub>2</sub> group. The strategy involves hybridizing isoniazid with various aromatic or heteroaromatic aldehydes, leading to the formation of a new functional group known as an imine. The selection of aromatic aldehydes as hybridization partners was motivated by their structural features. Compared to chains, aromatic aldehydes exhibit fewer degrees of freedom, which can contribute to enhanced ligand-receptor binding energy by reducing the entropic penalty. This property can potentially lead to increased compound potency (Mushtaque & Rizvi, 2023; Rohilla et al., 2024).

The designed compounds possess several key features:

- 1) Nucleophilic imine and reactive nitrogen: The imine group and the nitrogen in the pyridine ring offer nucleophilic sites for potential interactions with biological targets.
- 2) Electrophilic and nucleophilic character of the imine carbon: The imine carbon's dual reactivity can facilitate interactions with both electron-rich and electron-deficient groups.
- 3) Tautomerism potential: A carbonyl group adjacent to the -NH- group in hydrazine allows for the possibility of tautomerism in certain cases.
- 4) Intramolecular and intermolecular interactions: The relative positioning of the NH group to the -C=N group can influence the propensity for intramolecular and intermolecular interactions, potentially enhancing binding to biological targets.

- 5) Smaller molecular weight: The reduced molecular weight of these derivatives compared to isoniazid may facilitate intracellular penetration, mimic endogenous substrates, and increase the likelihood of interactions with various targets.

The structural modifications introduced in these compounds are expected to significantly influence their physicochemical properties, including lipophilicity, electronic characteristics, and steric effects. These alterations may, in turn, lead to changes in biological activity and therapeutic potential. Ultimately, the goal of these modifications is to improve the compounds' efficacy, particularly for applications as DNA-binding agents.

### Physicochemical and drug-likeness properties predictions

Prediction of the physicochemical properties of drug candidates is essential for efficient drug development and understanding their biological and medicinal actions (Leeson & Young, 2015; Meanwell, 2011). Properties such as molecular weight, the number of rotatable bonds, and the number of heavy atoms are integral to evaluating drug-likeness, helping identify oral drug candidates in the early phases of drug discovery (Lee et al., 2022a; Tripathi & Ayyannan, 2018). Drug-like compounds are molecules that contain functional groups and/or have physical properties consistent with the majority of known drugs, suggesting that these compounds could potentially exhibit biological activity or therapeutic effects. The drug-like characteristics serve as a parameter in choosing a more promising compound as a lead from the extensive combinatorial libraries (Lee et al., 2022b; Tian et al., 2015).

One of the foundational methods for assessing drug-like properties is Lipinski's Rule of Five (Ro5), developed by Pfizer's medicinal chemist, Christopher Lipinski. The RO5 was derived from an analysis of orally available drugs and clinical candidates, though it excludes certain classes

such as antibiotics, antifungals, vitamins, and cardiac glycosides. The RO5 states that a compound is more likely to be membrane permeable and easily absorbed via passive diffusion in human intestine if it meets the following criteria: molecular weight (MW) <500, The number of hydrogen bond donors (HBDs) <5 (counting the sum of all NH and OH groups), partition coefficient octanol/water Log P < 5, The number of hydrogen bond acceptors (HBAs) <10 (counting all N and O atoms). The thresholds in the rule are multiples of five, hence the name "Rule of Five" (Lipinski, 2004; Lipinski et al., 2001). Veber et al. (2002) expanded upon the Ro5 by identifying two additional descriptors crucial for optimal oral bioavailability in rats: the number of rotatable bonds (NBR) < 10 and polar surface area (PSA) < 140 Å<sup>2</sup> (Veber et al., 2002). According to the literature, if a compound violates two or more of the Ro5 properties, it is likely to be classified as non-drug-like or suitable for non-oral delivery routes (Lipinski et al., 2001; Sampat et al., 2022). Lipinski's Rule aids in filtering out compounds that are less likely to be of interest in ongoing research (Roman et al., 2023).

Molinspiration web-based software plays a pivotal role in evaluating physicochemical properties and drug-likeness. This tool leverages advanced Bayesian statistical methods, integrating the structural and property data of both active and inactive compounds to identify substructural features characteristic of biologically active molecules. The software calculates key physicochemical parameters crucial for predicting the theoretical oral bioavailability of the compounds under investigation. These parameters include molecular weight, partition coefficient (logP), the number of hydrogen bond acceptors and donors, the number of rotatable bonds, and total polar surface area, as outlined in Table 4A.

#### Number of heavy atoms (N atoms):

The number of heavy atoms in a molecule is a key factor in drug design, influencing molecular size, complexity, drug-likeness, and pharmacokinetic properties (García-Sosa et al., 2012). While larger molecules offer increased binding potential, they may also pose challenges related to synthesis, solubility, and membrane permeability. During lead optimization, reducing the number of heavy atoms can lower molecular weight and improve solubility, enhancing the drug-likeness profile without significantly affecting potency (de Souza Neto et al., 2020; Wang et al., 2019). Isoniazid derivatives contain between 16 and 24 heavy atoms, with INH having the lowest count at 10 atoms. The increase in heavy atoms in derivatives is often due to the substitution of larger aromatic rings or additional functional groups, such as in INH14, which has the highest count due to the inclusion of a naphthalene ring and a dimethylamino group.

#### Molecular weight (MW):

Molecular weight is the sum of the atomic weights of all atoms in a molecule, typically expressed in Daltons (Da) or grams per mole (g/mol). MW is a critical determinant of a drug's absorption, distribution, metabolism, and excretion (ADME) profile (Komura et al., 2023). As MW increases, drug permeability and absorption generally decrease, particularly concerning membrane permeability and penetration through the blood-brain barrier (BBB) (Pardridge, 2012). Additionally, drug clearance through artificial membranes inversely correlates with MW (Lienx & Wang, 1980). The MW values of the designed compounds range from 215.21 to 318.38 Da, all of which are under the 500 Da threshold, suggesting that these molecules are likely to be easily absorbed and exhibit good permeability across cell membranes.

#### Partition coefficient (LogP):

The partition coefficient is a key measure of lipophilicity or hydrophobicity, calculated as the logarithm of the concentration ratio of a compound between organic (usually n-octanol) and aqueous phases (Ruiz-García et al., 2008). Positive values of the partition coefficient suggest a tendency towards a lipophilic or hydrophobic environment, whereas negative values indicate a preference for a lipophobic or hydrophilic environment (Khanna & Ranganathan, 2009). LogP values significantly impact various ADMET parameters, drug-receptor interactions, and the overall potency of molecules (Tshepelevitch

et al., 2020). Compounds exhibiting extremely high or low LogP values may encounter challenges related to permeability and solubility (Waring, 2010). Highly hydrophilic compounds generally struggle to diffuse passively through cellular membranes due to their inability to penetrate the hydrophobic core of the lipid bilayer. Conversely, excessively lipophilic compounds may also face difficulties in membrane permeation, as they tend to become sequestered within the bilayer, impeding their effective transit (Lagorce et al., 2017). Researchers have also identified a correlation between a compound's logP value and its ability to penetrate the blood-brain barrier (BBB), a crucial factor for central nervous system (CNS) activity. For CNS-active drugs, a logP value in the range of 4 to 5 is generally considered optimal (Abraham et al., 1993; Feher et al., 2000). The LogP values for the designed compounds (INH01–INH19) were within the acceptable range per Lipinski's Rule and showed superior lipophilicity compared to the precursor compound, isoniazid (INH), which had a negative LogP value. This enhancement in lipophilicity, likely attributed to the presence of the Imine group and aromatic portion of the aldehyde, suggests enhanced absorption through biological membranes.

#### Hydrogen bond acceptor and hydrogen bond donor groups:

Hydrogen bonds play a crucial role in molecular recognition (Morozov & Kortemme, 2005; Santos-Martins & Forli, 2020), structural stability (Pace et al., 2011), enzyme catalysis (Calixto et al., 2019; Neves et al., 2017), and drug partition and permeability (Rezai et al., 2006; Shinoda, 2016). The presence of functional groups capable of forming hydrogen bonds can enhance a drug's solubility and its ability to interact with biomolecular targets, thereby influencing binding affinity and selectivity. However, an excess of hydrogen bond donors or acceptors can negatively impact membrane permeability and partitioning (Alex et al., 2011). In that regard, drug-like character predictors, such as Lipinski's rule of five (Ro5) have been using the number of hydrogen bond donors/acceptors as a molecular descriptor. In the designed compounds, the number of HBAs ranges from 4 to 8, and the number of HBDs ranges from 1 to 2, all within the limits set by the Ro5, ensuring that the hydrogen bonding potential does not compromise the compounds' drug-like properties.

#### The number of rotatable bonds (N roth):

The number of rotatable bonds is a measure of molecular flexibility and is an important descriptor for predicting oral bioavailability. A rotatable bond is defined as any single bond not part of a ring and bound to a non-terminal heavy atom (Veber et al., 2002). A higher number of rotatable bonds increases molecular flexibility, potentially improving binding affinity with target proteins. However, compounds with fewer rotatable bonds are generally more rigid, which can enhance oral bioavailability by reducing the entropy cost of binding (Vieth et al., 2004). In the designed compounds, the number of rotatable bonds does not exceed 10, which is favorable for maintaining good oral bioavailability.

#### Topological polar surface area (TPSA):

Topological polar surface area is a key descriptor related to hydrogen bonding and is important for drug transport properties such as intestinal absorption, BBB penetration, and oral bioavailability (Leeson, 2016; Veber et al., 2002). TPSA is calculated as the sum of the surface areas of polar atoms, primarily oxygen, and nitrogen, including attached hydrogens (Ertl et al., 2000). Therefore, TPSA is a reliable indicator of a compound's hydrogen bonding capacity. Compounds with a TPSA below 140 Å<sup>2</sup> typically exhibit good permeability and oral absorption, while those with a TPSA below 80 Å<sup>2</sup> are more likely to permeate the CNS by passive diffusion (Clark, 2011). The TPSA values for the isoniazid derivatives range from 54.59 to 109.14 Å<sup>2</sup>, well below the 140 Å<sup>2</sup> threshold, suggesting favorable absorption characteristics.

#### Molecular volume (Å<sup>3</sup>):

Molecular volume, a fundamental property of a molecule, plays a pivotal role in drug discovery. Its significance extends to optimizing drug candidates, understanding interactions with biological targets, and predicting pharmacokinetic properties (Flatow et al., 2014). By

determining the molecular volume of a compound, researchers can gain insights into its binding affinity, solubility, permeability, and overall drug-likeness (La-Scalea et al., 2005; Mcgowan, 1956). In the context of isoniazid derivatives, molecular volume variations offer valuable information. The range of molecular volumes observed in these derivatives, from 187.51 Å<sup>3</sup> to 295.84 Å<sup>3</sup>, highlights the influence of structural modifications on the overall molecular size and shape. This understanding can inform the design of novel derivatives with improved properties.

### Bioactivity predictions

In drug discovery, predicting the bioactivity of compounds against specific biological targets is crucial for understanding their potential therapeutic effects and toxicity profiles. Biological targets, which commonly include proteins, whether cytosolic, or membrane-embedded, and nucleic acids, play a key role in mediating the biological activity of drugs (Decherchi & Cavalli, 2020). To assess the likelihood of compounds interacting with these targets, bioactivity scores can be calculated using tools like Molinspiration, an open-source cheminformatics platform. These scores provide valuable insights into compounds' binding affinity and selectivity, facilitating the development of new drugs with enhanced efficacy and reduced side effects. Bioactivity scores are categorized as follows: compounds with scores greater than 0.0 are likely to exhibit significant biological activity, scores between -0.50 and 0.00 suggest moderate activity, and scores below -0.50 indicate inactivity (Khan et al., 2017). Table 4B suggests the compounds exhibit moderate to inactive interactions with six protein targets. The efficiency of bioactivity scores typically follows the order of Enzyme Inhibitors (EI), Kinase Inhibitors (KI), G-protein-coupled receptors (GPCR), Protease Inhibitors (PI), Nuclear Receptors (NRC), and Ion Channel Modulators (ICM). The bioactivity profiles of isoniazid derivatives (INH01 to INH19) vary significantly depending on the structural modifications made to the pyridine-4-carbohydrazide core. For instance, the parent compound, isoniazid, shows relatively low bioactivity scores across all six targets, particularly in the categories of Nuclear Receptors (NRC: -2.33) and Ion Channel Modulators (ICM: -1.45). This suggests a low predicted affinity for these targets, consistent with isoniazid's primary role as an antibiotic rather than a modulator of these pathways. Derivatives such as INH01 (Phenylmethylidene) exhibit moderate activity across all targets, indicating that simple phenyl substitution does not dramatically alter activity compared to the parent compound. In contrast, derivatives like INH13 (Furan-2-yl) and INH16 (Thiophen-2-yl), which feature heterocyclic aromatic rings, display the lowest activity scores, implying that these substitutions may lead to reduced bioactivity. The presence of sulfur in the thiophene ring of INH16 could contribute to an electron-rich environment that is less favorable for target interactions. Compounds with strong electron-withdrawing groups, such as INH03 (3-Nitrophenyl) and INH17 (2-Nitrophenyl), show decreased bioactivity across all targets, particularly for ICM and NRC. This suggests that the electron-withdrawing nature of the nitro group reduces binding affinity. Conversely, electron-donating groups like methoxy and hydroxy in derivatives such as INH05 (4-Hydroxy-3-methoxyphenyl) and INH11 (2-Hydroxy-5-methoxyphenyl) slightly improve bioactivity, possibly by enhancing electronic interactions with certain targets. Derivatives with dimethylamino groups, such as INH07 (4-Dimethylaminobenzylidene) and INH14 (4-(Dimethylamino)naphthalen-1-yl), show moderate activity, indicating that electron-donating groups can enhance bioactivity, though the overall effect also depends on the position and presence of additional substituents. Meanwhile, bulky naphthalene-containing derivatives like INH09 (2-Hydroxynaphthalen-1-yl) and INH19 (Naphthalen-2-yl) generally exhibit low bioactivity, likely due to increased steric hindrance that reduces effective target binding. Lastly, INH18 ((Z)-3-phenylprop-2-enylidene) shows moderate bioactivity, suggesting that some flexibility in molecular structure can slightly improve target binding, though not significantly.

### PASS prediction

The Prediction of Activity Spectra for Substances (PASS) platform provides a robust computational approach for forecasting the biological activity spectra of chemical compounds. Developed by the V. N. Orechovich Institute of Biomedical Chemistry, PASS predicts pharmacological effects based on structural similarities to known biologically active compounds. This model relies on a vast dataset, primarily derived from the MDL Drug Data Report (MDDR), and continuously updated to reflect discoveries in medicinal chemistry (Parasuraman, 2011).

The interpretation of PASS predictions requires a degree of flexibility, particularly concerning the values of Pa. A Pa value greater than 0.7 indicates a strong probability that the predicted biological activity can be experimentally confirmed. This suggests that the compound shares significant structural similarities with known pharmacologically active agents, making it a promising candidate for experimental validation. For Pa values between 0.5 and 0.7, the probability of experimental confirmation is lower. However, such compounds may exhibit novel structural features that are not closely aligned with known drugs. These novel features could offer valuable insights into unique or less common mechanisms of action. In contrast, a P value below 0.5 suggests a relatively low probability of experimental validation. Nonetheless, compounds with low Pa values may still exhibit structural novelty, presenting opportunities for discovery in previously unexplored areas of biological activity (Filimonov et al., 2014). Table 5 presents the PASS predictions for a series of pyridine-4-carbohydrazide derivatives (INH01–INH19), focusing on the most promising activities where Pa > 0.7. These predictions aim to understand the potential therapeutic applications of these compounds, with isoniazid (INH) serving as the template compound. Based on the data, each compound has multiple potential activities, we can classify the activities into several categories:

**Core Activities:** These activities appear consistently across multiple INH compounds and likely represent the primary mechanisms of action: antituberculosis, antimycobacterial, taurine dehydrogenase inhibitor, and amine dehydrogenase inhibitor.

**Secondary Activities:** These are activities that appear in multiple INH compounds but with less frequency or probability than the core activities. HMGCS2 expression enhancer (cholesterol metabolism), phosphatidylserine decarboxylase inhibitor (cell signaling), glutamine-phenylpyruvate transaminase inhibitor (amino acid metabolism), antiviral (picornavirus and poxvirus), beta-adrenergic receptor kinase inhibitor (hormonal signaling).

**Tertiary Activities:** These are less common and often have lower probabilities. Threonine aldolase inhibitor, isopenicillin-N epimerase inhibitor, nicotinamidase inhibitor, PFA-M1 aminopeptidase inhibitor, MCL-1 antagonist, nicotinic alpha6beta3beta4alpha5 receptor antagonist, corticosteroid side-chain-isomerase inhibitor, phenylalanine (histidine) transaminase inhibitor, CYP2A8 substrate, gluconate 2-dehydrogenase (acceptor) inhibitor, cytoprotectant, transcription factor stat3 inhibitor, arylalkyl acylamidase inhibitor, aldehyde dehydrogenase (pyrroloquinoline-quinone) inhibitor, thiol protease inhibitor, neuropeptide y2 antagonist, aspartate-phenylpyruvate transaminase inhibitor, phthalate 4,5-dioxygenase inhibitor, glycosylphosphatidylinositol phospholipase D inhibitor. Additionally, the analysis of predicted activities across the INH derivatives reveals some interesting structure-activity relationships (SARs). Antibacterial activity, a primary focus due to INH's established efficacy against Mycobacterium tuberculosis and Gram-positive bacteria, showed that many derivatives had comparable or even superior potency to INH. Structural modifications appear to enhance antibacterial potency, especially with para-substitution on the phenyl ring, which was particularly effective for antimycobacterial activity. Derivatives such as INH04, INH07, INH08, INH12, and INH15 exhibited higher activity with para-substituted phenyl groups. Electron-donating groups (e.g., -OCH<sub>3</sub>, -N(CH<sub>3</sub>)<sub>2</sub>) further improved activity, as seen in INH07, INH08, and INH14, while electron-

withdrawing groups (e.g., -NO<sub>2</sub>, -Cl) also boosted potency, as observed in INH03 and INH12. Compounds containing furan (INH13) or thiophene (INH16) substituents showed strong antibacterial activity, particularly against tuberculosis. In contrast, ortho- or meta-substitution (INH02, INH05, INH06, INH11) tended to reduce activity compared to para-substituted compounds. Naphthyl substitutions at the 1- or 2-position (INH09, INH14, INH19) did not significantly enhance activity over phenyl derivatives, and the lack of activity in INH14 suggests that bulkier groups may interfere with key binding interactions. Regarding antiviral activity, isoniazid itself demonstrated no potential across viral targets. However, many derivatives exhibited enhanced antiviral properties, underscoring the importance of structural modifications. Derivatives such as INH01, INH03, INH04, INH07, INH08, INH10, INH12, INH15, INH17, and INH19 displayed notable antiviral activity, with INH01, INH07, INH08, INH12, and INH15 showing efficacy against Picornavirus (PV) and Poxvirus (POV). Similar to the antibacterial SARs, para-substitution on the phenyl ring was again favored for antiviral activity. Electron-donating groups (e.g., -OCH<sub>3</sub>, -N(CH<sub>3</sub>)<sub>2</sub>) boosted activity in compounds like INH07, INH08, and INH14, while electron-withdrawing groups (e.g., -NO<sub>2</sub>, -Cl) enhanced activity in INH03 and INH12. Furan (INH13) and thiophene (INH16) substituents showed little antiviral activity, while ortho- or meta-substituted phenyl groups (INH02, INH05, INH06, INH11) performed less effectively. Naphthyl substituents (INH09, INH14, INH19) were not advantageous compared to phenyl groups. INH04, INH07, INH08, INH12, and INH15 emerge as promising candidates for further investigation, warranting *in vitro* and *in vivo* studies to confirm their antiviral efficacy and safety. In contrast, INH demonstrated no predicted activity as an enhancer of HMGCS2 expression, a key enzyme in lipid metabolism. However, many derivatives showed increased activity in this area, indicating that structural modifications improved the HMGCS2 expression-enhancing properties. Para-substitution on the phenyl ring was again advantageous for enhancing HMGCS2 expression. Compounds such as INH04, INH07, INH08, INH12, and INH15 showed heightened activity, with electron-donating groups (e.g., -OCH<sub>3</sub>, -N(CH<sub>3</sub>)<sub>2</sub>) further enhancing efficacy, as in INH07, INH08, and INH14. Electron-withdrawing groups (e.g., -NO<sub>2</sub>, -Cl) also proved beneficial, as seen in INH03 and INH12. INH13, containing a furan substituent, exhibited the highest activity for HMGCS2 expression enhancement, underscoring the importance of this group. As with antibacterial and antiviral activities, ortho- and meta-substitutions (INH02, INH05, INH06, INH11) resulted in reduced activity, while naphthyl substituents (INH09, INH14, INH19) did not significantly improve activity over phenyl groups. Derivatives INH02, INH10, INH12, and INH13 are particularly promising for further exploration in metabolic or transcriptional pathways regulated by HMGCS2.

#### ADME prediction

As opposed to pharmacodynamics, which describes what the drug does to the body. Pharmacokinetics (PK) describes what the body does to the drug (Currie, 2018a). There are four major determinants of PK, commonly called ADME properties (absorption, distribution, metabolism, and excretion). These properties are crucial for determining the drug's efficacy and safety (Lucas et al., 2019).

The ADME process can be broadly summarized as (i) drug dissolution in the gastrointestinal tract, followed by absorption through the gut wall and passage into the bloodstream via the liver; (ii) distribution of the drug to various tissues, depending on its structural and physicochemical properties; (iii) metabolism, where the drug is biochemically modified into metabolites, often by enzymatic systems, and (iv) elimination of the drug, usually through excretion (Gleeson et al., 2011; van de Waterbeemd & Gifford, 2003). For a compound to be effective it must reach its target in the body at sufficient concentrations and remain in a bioactive form long enough to exert its intended biological effects. Thus, understanding ADME properties early in drug development can help minimize the time, cost, and labor involved by focusing on compounds with promising profiles. This section evaluates the absorption,

distribution, metabolism, and excretion characteristics of pyridine-4-carbohydrazide derivatives (INH01–INH19), comparing them to the parent compound isoniazid (INH).

#### (A) Absorption

Absorption refers to the process by which a drug moves from the site of administration into systemic circulation (Currie, 2018b). Several parameters are used to evaluate the absorption potential of drug candidates: water solubility (LogS), human intestinal absorption (HIA), permeability across the Caco-2 cell line (LogPapp), skin permeability (LogKp), and their interactions with P-glycoprotein (P-gp I, II). These factors influence the bioavailability of a compound, especially when administered orally. The results of these parameters are summarized in Table 6A.

**Water solubility (logS):** Water solubility is critical for drug formulation and absorption, particularly for oral delivery (Barrett et al., 2022; Delaney, 2004). Low solubility can lead to poor bioavailability and impaired absorption, while high solubility can enhance drug dissolution and plasma concentration (Tran et al., 2023). The aqueous solubility of a substance is often expressed as log units of molar solubility (mol/L), or logS. The pyridine-4-carbohydrazide derivatives exhibit varying degrees of water solubility, ranging from -1.8896 to -4.042. Negative values reflect lower solubility. For example, INH01 (-2.076) and INH02 (-2.894) exhibit better solubility than isoniazid (-1.6), possibly due to simpler aromatic substitutions like phenyl (INH01) or hydroxyl groups (INH02), which slightly decrease solubility without significantly impairing absorption. On the other hand, derivatives like INH10 (-4.02), INH14 (-4.042), and INH17 (-3.643) show poor solubility, likely because of bulky or electron-withdrawing groups, such as nitro or naphthyl rings, which hinder aqueous solubility. These low solubility values suggest that these derivatives may struggle with absorption, particularly in aqueous environments.

**Human intestinal absorption (HIA):** HIA reflects how well a compound is absorbed through the intestinal lining (Azman et al., 2022), and a value over 80% is considered indicative of good absorption (Chander et al., 2017; Pires et al., 2015). The HIA values for the pyridine-4-carbohydrazide derivatives range from 83.21% to 96.43%, indicating that all compounds have good predicted absorption and are favorable for oral bioavailability. INH05 (96.317%) and INH14 (96.436%) show the highest absorption rates, suggesting that their methoxy-hydroxyphenyl and dimethylamino-naphthyl groups, respectively, enhance lipophilicity and passive diffusion through cell membranes. Conversely, INH10 (83.223%) and INH03 (85.889%) demonstrate lower absorption due to the presence of nitro groups, which tend to reduce membrane permeability. Isoniazid itself shows a lower HIA value (75.651%), likely due to its simple structure and lack of lipophilic substituents that facilitate passive absorption.

**The Caco-2 cell line (Caco-2):** The Caco-2 cell line is often used as a model for intestinal permeability (Kus et al., 2023). Compounds with a LogPapp value greater than 0.90 cm/s are considered to have high permeability (Pires et al., 2015). The pyridine-4-carbohydrazide derivatives show varying permeability values, ranging from -0.1 to 1.386. Compounds such as INH04, INH06, INH07, and INH09 exhibit high permeability, while others, including INH02, INH03, INH10, INH12, INH13, INH14, and INH17, show lower permeability. The reduced permeability of these compounds may be attributed to the presence of polar, bulky, or electron-withdrawing groups, which can impede passive diffusion across intestinal membranes.

**Skin permeability (LogKp):** Skin permeability reflects the ability of a drug to penetrate the skin barrier, a critical factor for transdermal drug delivery systems (Cordery et al., 2017; Pensado et al., 2022; Tsakovska et al., 2017). Compounds with a LogKp value greater than -2.5 cm/h are considered to have relatively low skin permeability (Pires et al., 2015). The LogKp values of the pyridine-4-carbohydrazide derivatives range from -3.29 to -2.398, suggesting limited potential for transdermal absorption in most compounds. However, INH18, with a LogKp value of

-2.398, exhibits the highest skin permeability among the derivatives, indicating that this compound may have potential for transdermal drug delivery.

**Permeability glycoprotein (P-gp) interaction:** P-gp is a membrane-bound efflux transporter that can limit the bioavailability of drugs by actively pumping them out of cells, particularly in tissues such as the intestines, liver, and brain (Saaby & Brodin, 2017). Compounds that are substrates for P-gp may face reduced bioavailability, as the transporter pumps them out of cells before they can reach therapeutic concentrations (Elmeliegy et al., 2020; Nielsen et al., 2023). Moreover, P-gp substrates can be further categorized into drugs that are not metabolized in humans and those that are substrates for both P-gp and drug-metabolizing enzymes, particularly CYP3A4. Given that many P-gp substrates are also metabolized by CYP3A4, and that P-gp inhibitors often inhibit CYP3A4 as well, numerous drug-drug interactions arise from the inhibition or induction of both P-gp and CYP3A4 (Fromm, 2004; König et al., 2013). Several compounds in the study, including INH03, INH07, INH08, INH09, and INH12, are predicted to be substrates for P-gp, suggesting they may face reduced bioavailability due to efflux and possible metabolism by CYP3A4. In contrast, isoniazid and the other derivatives are not expected to interact with P-gp, which may result in better bioavailability by avoiding efflux. Additionally, most compounds are not predicted to inhibit P-gp, except for INH14, which inhibits both P-gp I and II. This inhibition could enhance bioavailability by preventing the efflux of co-administered drugs, making INH14 a potential candidate for combination therapies aimed at overcoming multidrug resistance, particularly in cancer treatments (Côte-Real et al., 2019; Dong et al., 2020; Waghay & Zhang, 2018).

#### (D) Distribution

Drug distribution refers to the reversible transfer of a drug within the body, from the bloodstream to various tissues (Berellini et al., 2009; Motl et al., 2006). It plays a crucial role in the ADMET process, as it influences the amount of drug that reaches target sites, affecting both efficacy and potential toxicity (Sun et al., 2022). The distribution properties of derivatives are evaluated using four key parameters: volume of distribution, fraction unbound, blood-brain barrier permeability, and central nervous system permeability, as shown in Table 6B.

**The Volume of Distribution (VD<sub>ss</sub>)** quantifies how extensively a drug disperses into body tissues relative to the bloodstream. Higher VD<sub>ss</sub> values (closer to positive) indicate a greater extent of tissue distribution (Hsu et al., 2021). According to Pires et al., a compound is considered to have good tissue distribution if its VD<sub>ss</sub> value exceeds 2.81 L/kg (log VD<sub>ss</sub> > 0.45) and poor distribution if it is below 0.71 L/kg (log VD<sub>ss</sub> < -0.15) (Pires et al., 2015). The VD<sub>ss</sub> values for the derivatives range from -0.432 to 0.212 Log L/kg, suggesting low to moderate tissue distribution. Notably, compounds such as INH02, INH07, INH08, INH09, INH14, INH15, and INH19 exhibit moderate tissue distribution, likely due to their aromatic structures, which enhance lipophilicity compared to isoniazid and other derivatives.

**Fraction Unbound (FU)** represents the proportion of a drug in the plasma that remains unbound to proteins, with only the unbound fraction being pharmacologically active (Seyfinejad et al., 2021). A higher FU indicates a greater portion of the drug available to exert therapeutic effects (Watanabe et al., 2018). The FU values for the derivatives range from 0.031 to 0.333, with lower FU values corresponding to higher protein binding. Compounds such as INH14, INH19, and INH09, which contain extensive aromatic substituents, and INH03, INH10, and INH17, which contain nitro groups, show lower FU values. In contrast, isoniazid demonstrates the highest FU (0.728), significantly greater than most derivatives, reflecting minimal protein binding and suggesting a higher bioavailability for interaction with target sites.

**Blood-Brain Barrier (BBB) Permeability** indicates a drug's ability to cross the BBB, a selective barrier that regulates the entry of substances into the brain (Crivori et al., 2000). Compounds with a LogBB > 0.3 are

considered capable of crossing the BBB easily, while those with a LogBB < -1.0 face significant barriers (Pires et al., 2015). Most pyridine-4-carbohydrazide derivatives demonstrate low BBB permeability, suggesting limited brain penetration. However, compounds INH15 and INH18 exhibit higher BBB permeability, indicating their potential for greater brain access.

**CNS Permeability (Log PS)** further evaluates the ability of these compounds to penetrate the central nervous system. Compounds with a Log PS > -2 are considered capable of CNS penetration, while those with a Log PS < -3 are unlikely to cross the CNS barrier (Pires et al., 2015). For the derivatives studied, only INH19 exhibits a Log PS lower than -2, suggesting it has poor CNS penetration. The remaining derivatives exhibit moderate CNS permeability (Log PS between -2 and -3). Isoniazid, with a Log PS of -3.022, shows one of the lowest CNS permeabilities, indicating it is less likely to penetrate the CNS effectively, which aligns with its hydrophilic structure.

#### 3.5.3 | (M) Metabolism

Drug metabolism is the process by which the body's enzymes chemically modify drug molecules. This is a vital defense mechanism against potential toxins, which are often lipid-soluble and can accumulate in the body. To facilitate excretion, these toxins are converted into more water-soluble metabolites. Most drug metabolism occurs in the liver, where enzymes called hepatic microsomal enzymes catalyze the breakdown process. The metabolic properties of pyridine-4-carbohydrazide derivatives were assessed by evaluating their potential as substrates and/or inhibitors of key cytochrome P450 (CYP) enzymes, which are essential detoxifying enzymes predominantly expressed in the liver (Zanger & Schwab, 2013). To date, 57 distinct CYP isoforms have been identified in humans, of which five—CYP1A2, CYP2C9, CYP2C19, CYP2D6, and CYP3A4—play pivotal roles in drug metabolism (Wei et al., 2024). The metabolic pharmacokinetic characteristics of the compounds are presented in Table 6C.

Among these isoforms, CYP3A4 and CYP2D6 are of particular clinical importance due to their significant involvement in the metabolism of various drugs. Inhibition of these enzymes can result in reduced drug clearance, elevated drug plasma concentrations, and potential adverse reactions. Conversely, if a compound serves as a substrate for these enzymes, it is likely to be efficiently metabolized, reducing the risk of side effects related to drug accumulation. Several pyridine-4-carbohydrazide derivatives, including INH01, INH03, INH04, INH07, INH08, and INH10, are identified as substrates for CYP3A4, indicating their likelihood of efficient metabolic processing by this enzyme, thereby reducing the risk of accumulation-related side effects. Furthermore, most derivatives exhibit no significant inhibition of CYP2D6, CYP2E1 and CYP3A4, which is advantageous, as it suggests a lower potential for drug-drug interactions and reduced risk of hepatotoxicity. Notably, INH18 acts as a dual substrate for both CYP3A4 and CYP2D6, further lowering the probability of metabolic interactions. Regarding CYP1A2, all derivatives except INH06 inhibit this isoform, potentially resulting in elevated plasma concentrations of co-administered drugs metabolized by CYP1A2 and increasing the risk of drug-drug interactions. The inhibition of CYP1A2 may be linked to the presence of electron-withdrawing substituents, such as nitro and halogen groups, on the aromatic rings of these compounds, which likely facilitate interaction with the enzyme's active site. About CYP2C8, most derivatives inhibit this enzyme, with the exceptions of INH07, INH12, INH13, INH15 and INH16, which do not exhibit inhibitory activity. The inhibition observed in other derivatives may be attributed to structural features, such as bulky substituents, which could impede the enzyme's binding affinity. For CYP2C9, only INH14 shows inhibitory activity, which may be ascribed to the presence of a dimethylaminonaphthyl group that interacts with the active site of CYP2C9. Several derivatives also exhibit inhibition of CYP2C19, including INH04, INH09, INH10, INH14, INH18, and INH19. Structural elements such as nitro groups in INH09 and INH10, and naphthyl groups in INH14 and INH19, likely contribute to this inhibitory activity by

introducing steric and electronic effects that influence binding to the CYP2C19 active site.

### (E) Excretion

Excretion refers to the process by which drugs are eliminated from the body, and it is closely related to the concentration of the drug in the bloodstream and the rate of elimination (Talevi & Bellera, 2018). In this study, the excretion properties of pyridine-4-carbohydrazide derivatives (INH01–INH19) were evaluated based on their total clearance ( $CL_{tot}$ ) values, expressed in Log ml/min/kg, and their potential interaction with the Renal Organic Cation Transporter 2 (OCT2), as presented in Table 6D. The total clearance ( $CL_{tot}$ ) values for the derivatives ranged from 0.027 to 0.966 Log ml/min/kg. Isoniazid, the reference compound, exhibited a moderate clearance rate (Log  $CL_{tot}$  = 0.782). Several derivatives showed clearance values close to this, suggesting that, despite structural modifications, the pyridine-4-carbohydrazide core structure contributes to a baseline level of metabolic stability. Derivatives with higher clearance rates (Log  $CL_{tot}$  > 0.800), represented in Tuscan color, include INH05, INH06, INH10, INH11, INH14, and INH18. These compounds are cleared more rapidly from the body, indicating potentially shorter half-lives and a possible need for more frequent dosing. Structural features such as electron-withdrawing groups (e.g., nitro groups in INH10 and INH11) or bulky aromatic substituents (e.g., the naphthyl group in INH14) likely enhance the compounds' interaction with metabolic enzymes, leading to increased clearance. In contrast, compounds INH01, INH02, INH03, INH07, INH08, INH09, INH12, INH13, INH15, INH17, INH19, and isoniazid exhibit moderate clearance rates (Log  $CL_{tot}$  ~ 0.700–0.800), indicated in green color. These derivatives typically feature less complex aromatic substitutions, which may reduce metabolic enzyme interactions, resulting in slower clearance rates. Compounds with moderate clearance rates are likely to remain in the body for a longer duration, which may enhance their ability to reach and maintain therapeutic levels at target sites. The lowest clearance rates (Log  $CL_{tot}$  < 0.700), represented in gray color, were observed for INH04 and INH16. INH04 contains a chlorine atom, while INH16 features a thiophene ring, both of which may reduce the compounds' susceptibility to metabolic breakdown and excretion, leading to lower clearance. Derivatives with low to moderate clearance may have extended half-lives, potentially increasing the risk of accumulation, but also offering the advantage of less frequent dosing. The role of OCT2 in renal clearance was also assessed. OCT2 is a key renal uptake transporter involved in the active secretion of drugs and endogenous compounds (Burkhardt & Wolff, 2000; Wright, 2019). Predicting whether a compound interacts with OCT2 is crucial for understanding its excretion pathway and potential contraindications (Lin et al., 2023). Based on pKCSM predictions, none of the derivatives, including isoniazid, were identified as OCT2 substrates. This suggests that these compounds are unlikely to be actively transported via OCT2, reducing the likelihood of their involvement in renal secretion (Bicker et al., 2020). Consequently, their clearance is more likely to be mediated through hepatic rather than renal pathways. This finding implies that renal toxicity and drug-drug interactions associated with OCT2 inhibition are not a major concern for these derivatives.

### Conclusion

In drug discovery, understanding and predicting the physicochemical properties of compounds is essential to optimize their pharmacokinetic profiles. The pyridine-4-carbohydrazide derivatives examined in this study show a clear trend of improved physicochemical properties compared to the parent compound, isoniazid (INH). These enhancements are attributed to the structural modifications involving diverse aromatic substituents, resulting in derivatives with varied molecular weight, volume, hydrophobicity and hydrogen bonding capacity. Crucially, all examined compounds meet the criteria of Lipinski's Rule of Five and the Veber rule, suggesting they possess favorable drug-likeness characteristics, high permeability and biological availability. Despite their increased molecular complexity, these compounds maintain drug-likeness without violations, reinforcing their potential as drug candidates. The

bioactivity scores of the derivatives demonstrate that structural modifications significantly influence predicted interactions with various biological targets. Unlike isoniazid, which exhibits limited bioactivity across a range of targets, derivatives with aromatic electron-donating groups showed improved bioactivity. On the other hand, the presence of electron-withdrawing groups tends to diminish the compounds' biological activity. This highlights the importance of careful structural modification to optimize bioactivity profiles, as the electronic properties of these groups directly impact target binding affinities. The PASS predictions for the pyridine-4-carbohydrazide derivatives provide key insights into the impact of structural modifications on their pharmacological potential. Compounds such as INH03, INH09, INH14 and INH19 show high predicted activity across various therapeutic categories, positioning them as strong candidates for further experimental investigation. These derivatives demonstrate potential in antibacterial, antiviral, antiprotozoal, anti-inflammatory and anticancer applications. The observed structural modifications create opportunities for the discovery of novel bioactive agents, offering promising avenues for the development of new therapeutic interventions across a range of medical fields.

The pharmacokinetic profiles of the pyridine-4-carbohydrazide derivatives also highlight the influence of structural modifications on absorption, distribution, metabolism and excretion. Many of the derivatives show improved absorption and permeability profiles compared to isoniazid, particularly those with electron-withdrawing or hydrophobic substituents. However, some derivatives face challenges such as limited solubility or interactions with P-glycoprotein (P-gp), necessitating further optimization to overcome these absorption barriers. In terms of distribution, bulky and lipophilic derivatives exhibit greater tissue penetration and blood-brain barrier permeability, suggesting their potential utility in treating CNS-related conditions. However, these modifications may also increase the risk of CNS side effects, requiring a balanced approach to design. Metabolic profiling highlights the influence of specific substituents on interactions with cytochrome P450 enzymes, with some derivatives, such as INH14, exhibiting enhanced CYP450 inhibitory activity. This underscores the need to carefully consider structural modifications to minimize drug-drug interaction risks. Excretion rates also vary, with derivatives showing different clearance values. Those with higher clearance rates may require more frequent dosing, while others with lower clearance could risk accumulation. The absence of renal OCT2 interactions suggests hepatic clearance pathways, reducing the risk of renal toxicity. Overall, while these derivatives show promising pharmacological and pharmacokinetic profiles, further optimization and experimental validation will be essential to fully realize their therapeutic potential.

### Declaration of Competing Interest

All authors have made significant contributions to this manuscript, as follows: (a) conception, design, analysis, and interpretation of the data; (b) drafting the manuscript or critically revising it for significant intellectual content and (c) approving the final version to be published.

**Sofian S. Mohamed** led the study's design, investigation, data interpretation, and initial drafting. **Salah M. Bensaber** provided supervision and contributed to the study design. **Nisreen H. Meiqal** and **Anton Hermann** participated in reviewing and editing the manuscript. **Abdul M. Gbaj** contributed through supervision, validation and drafting of the manuscript.

All authors have reviewed and approved the final version of the manuscript. The authors confirm that this manuscript has not been submitted to, nor is it under review at, any other journal or publication venue.

### Acknowledgments

We would like to thank the team of Judicial Expertise and Research Center, Tripoli, Libya for technical support throughout this project. We also thank Sir consultant Khaled Abuajila Diab (CEO of Judicial Expertise and Research Center, Tripoli, Libya) for his valuable support while performing this project.

### Ethical approval

All the methods were performed under relevant institutional guidelines and regulations.

### Appendix A. Supplementary material

Supplementary data associated with this article can be found in the online at [XXXXXXX].

### Supplementary material

Codes	N atoms	Lipinski's Rule				Veber Rule		N violations of rule of 5	Volume (Å <sup>3</sup> )
		MW (Da)	mi logP	N ON	N OHNH	N rotb	TPSA (Å <sup>2</sup> )		
INH01	17	225.25	1.81	4	1	3	54.35	0	205.94
INH02	18	241.25	1.75	5	2	3	74.58	0	213.94
INH03	20	270.25	1.74	7	1	4	100.18	0	229.28
INH04	18	259.70	2.26	4	1	3	54.35	0	219.48
INH05	20	268.32	1.91	5	1	4	54.59	0	239.51
INH06	21	255.28	1.87	5	1	4	54.59	0	256.31
INH07	20	271.28	1.15	6	2	4	83.82	0	251.85
INH08	19	285.30	1.15	6	2	5	83.82	0	231.49
INH09	22	291.31	2.91	5	2	3	74.58	0	257.95
INH10	22	300.27	1.75	8	1	5	109.14	0	254.82
INH11	20	271.28	1.78	6	2	4	83.82	0	239.51
INH12	20	270.25	1.77	7	1	4	100.18	0	229.28
INH13	16	215.21	1.07	5	1	3	67.49	0	187.51
INH14	24	318.38	3.02	5	1	4	57.59	0	295.84
INH15	18	239.28	2.26	4	1	3	54.35	0	222.50
INH16	16	231.28	1.71	4	1	3	54.35	0	196.65
INH17	20	270.25	1.72	7	1	4	100.18	0	229.28
INH18	19	251.29	2.03	4	1	4	54.35	0	233.63
INH19	21	275.31	2.99	4	1	3	54.35	0	249.93
INH	10	137.14	-0.97	4	3	1	68.01	0	122.65

**Table 4A:** Physicochemical Properties and Drug-Likeness Scores for the Predicted Compounds.

**Abbreviations:** Number of nonhydrogen atoms (N atoms); Molecular Weight (MW); Logarithm of partition Coefficient Between n-octanol and water LogP); Number of hydrogen bond acceptors (N-ON,O, and N atoms); Number of Hydrogen Bond Donors (N-OHNH,OH, and NH

groups); Number of Rotatable Bonds (N-rotb), Topological Polar Surface area (TPSA); and Number of violations (N violations); Number of violations (N violations); and Molecular volume (Å<sup>3</sup>).

Codes	Bioactivities score					
	EI	KI	GPCR	PI	NRC	ICM
INH01	-0.49	-0.59	-0.65	-0.93	-1.02	-0.87
INH02	-0.40	-0.49	-0.53	-0.75	-0.77	-0.9
INH03	-0.52	-0.54	-0.62	-0.83	-0.84	-0.82

INH04	-0.48	-0.55	-0.55	-0.88	-0.94	-0.81
INH05	-0.38	-0.32	-0.42	-0.68	-0.69	-0.77
INH06	-0.45	-0.47	-0.54	-0.8	-0.81	-0.87
INH07	-0.36	-0.36	-0.44	-0.75	-0.66	-0.79
INH08	-0.38	-0.38	-0.43	-0.7	-0.57	-0.78
INH09	-0.3	-0.27	-0.31	-0.48	-0.48	-0.67
INH10	-0.54	-0.47	-0.54	-0.73	-0.75	-0.90
INH11	-0.33	-0.40	-0.54	-0.66	-0.61	-0.90
INH12	-0.50	-0.54	-0.61	-0.83	-0.83	-0.80
INH13	-0.77	-1.00	-0.98	-1.25	-1.55	-1.06
INH14	-0.23	-0.17	-0.11	-0.40	-0.38	-0.58
INH15	-0.51	-0.56	-0.62	-0.90	-0.94	-0.91
INH16	-0.70	-0.99	-1.01	-1.12	-1.48	-1.24
INH17	-0.59	-0.63	-0.67	-0.84	-0.77	-0.83
INH18	-0.31	-0.64	-0.35	-0.65	-0.79	-0.81
INH19	-0.29	-0.26	-0.31	-0.50	-0.59	-0.68
INH	-0.66	-1.05	-1.39	-1.23	-2.33	-1.45

**Table 4B:** Bioactivity score of compounds according to Molinspiratin cheminformatics.

**Abbreviations:** G protein-coupled receptor (GPCR) ligand, Ion channel modulator (ICM), Kinase inhibitor (KI), Nuclear receptor ligand (NRL), Protease inhibitor (PI), Enzyme inhibitor (EI). The gray color represents

inactive and the green color represents moderate bioactivity under the scores reflect the predicted bioactivity, with more negative values indicating lower predicted activity for a given target.

Codes	Probability of Activity (Pa)	Probability of Activity (Pi)	Therapeutic Activity
NH01	0,913	0,002	Glutamine-phenylpyruvate transaminase inhibitor
	0,908	0,004	Taurine dehydrogenase inhibitor
	0,895	0,003	Amine dehydrogenase inhibitor
	0,880	0,003	Threonine aldolase inhibitor
	0,860	0,002	Antituberculosic
	0,855	0,004	HMGCS2 expression enhancer
	0,853	0,003	Isopenicillin-N epimerase inhibitor
	0,851	0,008	Beta-adrenergic receptor kinase inhibitor
	0,851	0,008	G-protein-coupled receptor kinase inhibitor
	0,840	0,003	Antimycobacterial
	0,822	0,002	Phenylalanine(histidine) transaminase inhibitor
	0,813	0,003	Antiviral (Picornavirus)
	0,812	0,004	Phosphatidylserine decarboxylase inhibitor
	0,776	0,003	PfA-M1 aminopeptidase inhibitor
	0,759	0,002	Serine-pyruvate transaminase inhibitor
0,748	0,003	Trimethylamine dehydrogenase inhibitor	

Codes	Probability of Activity (Pa)	Probability of Activity (Pi)	Therapeutic Activity
	0,743	0,003	Nicotinamidase inhibitor
	0,743	0,004	Mcl-1 antagonist
	0,734	0,008	Antiviral (Poxvirus)
	0,720	0,029	Nicotinic alpha6beta3beta4alpha5 receptor antagonist
NH02	0,901	0,002	Antituberculosic
	0,900	0,002	Threonine aldolase inhibitor
	0,897	0,004	Taurine dehydrogenase inhibitor
	0,891	0,003	Amine dehydrogenase inhibitor
	0,872	0,003	HMGCS2 expression enhancer
	0,866	0,003	Antimycobacterial
	0,862	0,003	Glutamine-phenylpyruvate transaminase inhibitor
	0,831	0,003	Phosphatidylserine decarboxylase inhibitor
	0,836	0,009	Beta-adrenergic receptor kinase inhibitor
	0,836	0,009	G-protein-coupled receptor kinase inhibitor
	0,769	0,003	Nicotinamidase inhibitor
	0,768	0,003	PfA-M1 aminopeptidase inhibitor
	0,767	0,004	Isopenicillin-N epimerase inhibitor
	0,725	0,004	Mcl-1 antagonist
	0,723	0,007	Corticosteroid side-chain-isomerase inhibitor
0,715	0,005	Antiviral (Picornavirus)	
0,709	0,004	Phenylalanine(histidine) transaminase inhibitor	
NH03	0,930	0,002	Antituberculosic
	0,896	0,003	Antimycobacterial
	0,863	0,002	Antiviral (Picornavirus)
	0,854	0,003	Phosphatidylserine decarboxylase inhibitor
	0,851	0,004	HMGCS2 expression enhancer
	0,839	0,008	Taurine dehydrogenase inhibitor
	0,801	0,003	Nicotinamidase inhibitor
	0,775	0,005	Glutamine-phenylpyruvate transaminase inhibitor
	0,747	0,005	Amine dehydrogenase inhibitor
	0,742	0,003	PfA-M1 aminopeptidase inhibitor
	0,737	0,004	Mcl-1 antagonist
NH04	0,909	0,003	Taurine dehydrogenase inhibitor
	0,881	0,003	Amine dehydrogenase inhibitor
	0,860	0,003	Glutamine-phenylpyruvate transaminase inhibitor
	0,844	0,003	Antituberculosic
	0,844	0,004	HMGCS2 expression enhancer
	0,839	0,003	Antimycobacterial
	0,804	0,013	G-protein-coupled receptor kinase inhibitor
	0,804	0,013	Beta-adrenergic receptor kinase inhibitor
	0,788	0,003	Antiviral (Picornavirus)

Codes	Probability of Activity (Pa)	Probability of Activity (Pi)	Therapeutic Activity
	0,782	0,005	Threonine aldolase inhibitor
	0,751	0,003	PfA-M1 aminopeptidase inhibitor
	0,709	0,005	Isopenicillin-N epimerase inhibitor
	0,705	0,004	Phenylalanine(histidine) transaminase inhibitor
	0,705	0,007	CYP2A8 substrate
	0,708	0,011	Phosphatidylserine decarboxylase inhibitor
	0,703	0,009	Antiviral (Poxvirus)
	0,748	0,055	Phobic disorders treatment
NH05	0,890	0,002	Antituberculosic
	0,871	0,003	Antimycobacterial
	0,846	0,004	Amine dehydrogenase inhibitor
	0,843	0,007	Taurine dehydrogenase inhibitor
	0,814	0,004	Threonine aldolase inhibitor
	0,760	0,007	HMGCS2 expression enhancer
	0,748	0,003	Cytoprotectant
	0,748	0,018	Beta-adrenergic receptor kinase inhibitor
	0,748	0,018	G-protein-coupled receptor kinase inhibitor
	0,727	0,009	Phosphatidylserine decarboxylase inhibitor
	0,721	0,009	Glutamine-phenylpyruvate transaminase inhibitor
NH06	0,913	0,002	Antituberculosic
	0,880	0,005	G-protein-coupled receptor kinase inhibitor
	0,880	0,005	Beta-adrenergic receptor kinase inhibitor
	0,873	0,003	Antimycobacterial
	0,752	0,006	Phosphatidylserine decarboxylase inhibitor
	0,736	0,004	Cytoprotectant
	0,727	0,008	Threonine aldolase inhibitor
	0,709	0,009	HMGCS2 expression enhancer
	0,706	0,030	Taurine dehydrogenase inhibitor
NH07	0,946	0,002	Taurine dehydrogenase inhibitor
	0,800	0,004	Antimycobacterial
	0,800	0,005	Glutamine-phenylpyruvate transaminase inhibitor
	0,797	0,003	Antituberculosic
	0,798	0,005	HMGCS2 expression enhancer
	0,787	0,005	Amine dehydrogenase inhibitor
	0,780	0,005	Threonine aldolase inhibitor
	0,759	0,006	Phosphatidylserine decarboxylase inhibitor
	0,752	0,004	Antiviral (Picornavirus)
	0,743	0,008	Antiviral (Poxvirus)
	0,719	0,021	Beta-adrenergic receptor kinase inhibitor
	0,719	0,021	G-protein-coupled receptor kinase inhibitor

Codes	Probability of Activity (Pa)	Probability of Activity (Pi)	Therapeutic Activity
<b>NH08</b>	0,895	0,003	Amine dehydrogenase inhibitor
	0,889	0,004	Taurine dehydrogenase inhibitor
	0,847	0,003	Antimycobacterial
	0,845	0,003	Antituberculosic
	0,811	0,012	Beta-adrenergic receptor kinase inhibitor
	0,811	0,012	G-protein-coupled receptor kinase inhibitor
	0,803	0,005	HMGCS2 expression enhancer
	0,800	0,005	Glutamine-phenylpyruvate transaminase inhibitor
	0,766	0,005	Threonine aldolase inhibitor
	0,747	0,004	Antiviral (Picornavirus)
	0,744	0,035	Gluconate 2-dehydrogenase (acceptor) inhibitor
	0,710	0,004	Cytoprotectant
<b>NH09</b>	0,865	0,005	Taurine dehydrogenase inhibitor
	0,864	0,003	Amine dehydrogenase inhibitor
	0,862	0,002	Antituberculosic
	0,851	0,003	Threonine aldolase inhibitor
	0,848	0,003	Antimycobacterial
	0,799	0,005	Glutamine-phenylpyruvate transaminase inhibitor
	0,792	0,005	HMGCS2 expression enhancer
	0,773	0,005	Phosphatidylserine decarboxylase inhibitor
	0,743	0,004	Isopenicillin-N epimerase inhibitor
	0,730	0,020	Beta-adrenergic receptor kinase inhibitor
	0,730	0,020	G-protein-coupled receptor kinase inhibitor
	0,710	0,004	Cytoprotectant
<b>NH10</b>	0,924	0,002	Antituberculosic
	0,904	0,002	Antimycobacterial
	0,865	0,003	HMGCS2 expression enhancer
	0,778	0,016	Taurine dehydrogenase inhibitor
	0,754	0,006	Phosphatidylserine decarboxylase inhibitor
	0,741	0,004	Transcription factor STAT3 inhibitor
	0,708	0,003	PfA-M1 aminopeptidase inhibitor
	0,708	0,005	Antiviral (Picornavirus)
<b>NH11</b>	0,891	0,002	Antituberculosic
	0,879	0,003	Amine dehydrogenase inhibitor
	0,874	0,003	Antimycobacterial
	0,863	0,005	Taurine dehydrogenase inhibitor
	0,839	0,004	HMGCS2 expression enhancer
	0,809	0,004	Threonine aldolase inhibitor
	0,792	0,014	G-protein-coupled receptor kinase inhibitor
	0,792	0,014	Beta-adrenergic receptor kinase inhibitor
	0,776	0,003	Cytoprotectant

Codes	Probability of Activity (Pa)	Probability of Activity (Pi)	Therapeutic Activity
	0,723	0,009	Phosphatidylserine decarboxylase inhibitor
	0,716	0,003	PfA-M1 aminopeptidase inhibitor
	0,714	0,009	Glutamine-phenylpyruvate transaminase inhibitor
	0,722	0,045	Gluconate 2-dehydrogenase (acceptor) inhibitor
NH12	0,928	0,002	Antituberculosic
	0,895	0,003	Antimycobacterial
	0,872	0,002	Phosphatidylserine decarboxylase inhibitor
	0,864	0,003	HMGCS2 expression enhancer
	0,862	0,005	Taurine dehydrogenase inhibitor
	0,854	0,003	Antiviral (Picornavirus)
	0,845	0,002	Nicotinamidase inhibitor
	0,823	0,004	Glutamine-phenylpyruvate transaminase inhibitor
	0,789	0,004	Amine dehydrogenase inhibitor
	0,762	0,004	Mcl-1 antagonist
	0,753	0,003	PfA-M1 aminopeptidase inhibitor
	0,718	0,008	Threonine aldolase inhibitor
	0,718	0,009	Antiviral (Poxvirus)
	0,718	0,040	Acrocyllindropepsin inhibitor
	0,718	0,040	Chymosin inhibitor
0,718	0,040	Saccharopepsin inhibitor	
NH13	0,956	0,001	HMGCS2 expression enhancer
	0,928	0,002	Antituberculosic
	0,913	0,003	Mcl-1 antagonist
	0,904	0,002	Antimycobacterial
	0,796	0,005	Glutamine-phenylpyruvate transaminase inhibitor
	0,792	0,003	Isopenicillin-N epimerase inhibitor
	0,791	0,004	Amine dehydrogenase inhibitor
	0,761	0,003	PfA-M1 aminopeptidase inhibitor
	0,748	0,003	Neuropeptide Y2 antagonist
	0,746	0,022	Taurine dehydrogenase inhibitor
	0,720	0,008	Threonine aldolase inhibitor
	0,707	0,004	Amyloid beta precursor protein antagonist
NH14	0,912	0,003	Taurine dehydrogenase inhibitor
	0,762	0,006	HMGCS2 expression enhancer
	0,702	0,008	Amine dehydrogenase inhibitor
NH15	0,889	0,004	Taurine dehydrogenase inhibitor
	0,876	0,003	Glutamine-phenylpyruvate transaminase inhibitor
	0,867	0,003	Amine dehydrogenase inhibitor
	0,866	0,002	Antituberculosic
	0,847	0,003	Antimycobacterial

Codes	Probability of Activity (Pa)	Probability of Activity (Pi)	Therapeutic Activity
	0,830	0,004	HMGCS2 expression enhancer
	0,808	0,004	Threonine aldolase inhibitor
	0,813	0,012	G-protein-coupled receptor kinase inhibitor
	0,813	0,012	Beta-adrenergic receptor kinase inhibitor
	0,804	0,003	Isopenicillin-N epimerase inhibitor
	0,804	0,004	Phosphatidylserine decarboxylase inhibitor
	0,761	0,004	Antiviral (Picornavirus)
	0,754	0,003	PfA-M1 aminopeptidase inhibitor
	0,740	0,004	Phenylalanine(histidine) transaminase inhibitor
	0,710	0,003	Serine-pyruvate transaminase inhibitor
	0,711	0,009	Antiviral (Poxvirus)
NH16	0,796	0,005	Glutamine-phenylpyruvate transaminase inhibitor
	0,771	0,004	CYP2E1 inhibitor
	0,761	0,004	Antimycobacterial
	0,759	0,004	Antituberculosic
	0,753	0,004	Mcl-1 antagonist
	0,747	0,022	Taurine dehydrogenase inhibitor
	0,721	0,003	PfA-M1 aminopeptidase inhibitor
NH17	0,861	0,005	Taurine dehydrogenase inhibitor
	0,845	0,004	HMGCS2 expression enhancer
	0,841	0,003	Phosphatidylserine decarboxylase inhibitor
	0,838	0,003	Antituberculosic
	0,809	0,004	Antimycobacterial
	0,800	0,005	Glutamine-phenylpyruvate transaminase inhibitor
	0,788	0,004	Amine dehydrogenase inhibitor
	0,783	0,004	Arylalkyl acylamidase inhibitor
	0,776	0,004	Aldehyde dehydrogenase (pyrroloquinoline-quinone) inhibitor
	0,768	0,003	Nicotinamidase inhibitor
	0,765	0,004	Antiviral (Picornavirus)
	0,734	0,003	Phenylalanine racemase (ATP-hydrolysing) inhibitor
0,708	0,009	Threonine aldolase inhibitor	
NH18	0,860	0,003	Glutamine-phenylpyruvate transaminase inhibitor
	0,841	0,004	Amine dehydrogenase inhibitor
	0,836	0,008	Taurine dehydrogenase inhibitor
	0,824	0,003	Antituberculosic
	0,807	0,004	Antimycobacterial
	0,802	0,004	Threonine aldolase inhibitor
	0,761	0,004	Thiol protease inhibitor
	0,750	0,004	Isopenicillin-N epimerase inhibitor
	0,726	0,009	Phosphatidylserine decarboxylase inhibitor
	0,710	0,004	Mcl-1 antagonist

Codes	Probability of Activity (Pa)	Probability of Activity (Pi)	Therapeutic Activity
	0,705	0,004	Phenylalanine(histidine) transaminase inhibitor
NH19	0,883	0,004	Taurine dehydrogenase inhibitor
	0,876	0,003	Glutamine-phenylpyruvate transaminase inhibitor
	0,861	0,003	Amine dehydrogenase inhibitor
	0,838	0,003	Isopenicillin-N epimerase inhibitor
	0,825	0,004	Threonine aldolase inhibitor
	0,825	0,004	HMGCS2 expression enhancer
	0,770	0,003	Antituberculosic
	0,753	0,004	Antimycobacterial
	0,751	0,006	Phosphatidylserine decarboxylase inhibitor
	0,740	0,004	Phenylalanine(histidine) transaminase inhibitor
	0,715	0,005	Antiviral (Picornavirus)
NH	0,968	0,001	Taurine dehydrogenase inhibitor
	0,926	0,001	Trimethylamine dehydrogenase inhibitor
	0,847	0,004	Amine dehydrogenase inhibitor
	0,842	0,003	Isopenicillin-N epimerase inhibitor
	0,825	0,004	Aldehyde dehydrogenase (pyrroloquinoline-quinone) inhibitor
	0,816	0,004	Arylalkyl acylamidase inhibitor
	0,810	0,003	Antituberculosic
	0,798	0,004	Antimycobacterial
	0,790	0,003	Nitrilase inhibitor
	0,782	0,002	Maillard reaction inhibitor
	0,781	0,014	Nicotinic alpha6beta3beta4alpha5 receptor antagonist
	0,761	0,001	Aralkylamine dehydrogenase inhibitor
	0,774	0,015	Glucose oxidase inhibitor
	0,754	0,008	Manganese peroxidase inhibitor
	0,757	0,013	Arylacetonitrilase inhibitor
	0,758	0,016	Nicotinic alpha2beta2 receptor antagonist
	0,738	0,004	N-methylhydantoinase (ATP-hydrolysing) inhibitor
	0,739	0,009	Nucleoside oxidase (H2O2-forming) inhibitor
	0,730	0,004	Nicotinate dehydrogenase inhibitor
	0,724	0,010	Peroxidase inhibitor
0,739	0,030	Nootropic	
0,713	0,008	Aspartate-phenylpyruvate transaminase inhibitor	
0,712	0,013	Phthalate 4,5-dioxygenase inhibitor	
0,716	0,031	Glycosylphosphatidylinositol phospholipase D inhibitor	
0,701	0,076	Phobic disorders treatment	

**Table 5:** PASS prediction Properties of the Predicted Compounds.

**Abbreviations:** Tuscan shading indicates the probability of activity values, and Gray represents the probability of inactivity values.

Codes	LogS	HIA	Caco-2	LogKp	P-gp subs	P-gp I Inhi	P-gp II Inhi
INH01	-2.076	93.954	1.329	-2.682	No	No	No
INH02	-2.894	93.974	0.745	-3.29	No	No	No
INH03	-3.641	85.889	-0.1	-2.67	Yes	No	No
INH04	-3.011	93.211	1.353	-2.677	No	No	No
INH05	-2.957	96.317	1.328	-2.767	No	No	No
INH06	-3.003	95.629	1.382	-2.713	No	No	No
INH07	-3.572	94.695	1.386	-3.06	Yes	No	No
INH08	-3.004	94.276	1.369	-3.048	Yes	No	No
INH09	-3.322	94.223	1.086	-2.778	Yes	No	No
INH10	-4.02	83.223	0.265	-2.742	No	No	No
INH11	-3.013	94.858	1.197	-2.909	No	No	No
INH12	-3.052	85.921	0.194	-2.68	Yes	No	No
INH13	-1.8896	95.967	0.801	-3.116	No	No	No
INH14	-4.042	96.436	-4.042	-2.678	No	Yes	Yes
INH15	-3.237	95.012	1.322	-2.568	No	No	No
INH16	-3.321	93.537	1.317	-2.694	No	No	No
INH17	-3.643	84.54	0.235	-2.79	No	No	No
INH18	-3.415	92.813	1.35	-2.398	No	No	No
INH19	-3.554	94.021	1.374	-2.518	Yes	No	No
INH	-1.6	75.651	0.627	-3.173	No	No	No

**Table 6A:** Absorption Properties of the Predicted Compounds.

**Abbreviations:** Water solubility (logS, log mol/L), Human Intestinal Absorption (HIA, %), Human colon epithelial cancer cell line (Caco-2, Log Papp; log cm/s), Skin permeability (LogKp; cm/h), Permeability glycoprotein I, II (P-gp I, II). Gray shading indicates low values, green represents moderate values, and Tuscan signifies high values. Pink shading and "Yes" denote an effect on the target, while white shading and "No" indicate no effect on the target.

Codes	VD <sub>ss</sub>	F <sub>u</sub>	LogBB	Log PS
INH01	-0.349	0.204	0.205	-2.252
INH02	-0.149	0.333	-0.184	-2.497
INH03	-0.232	0.076	-0.518	-2.484
INH04	-0.276	0.203	0.146	-2.141
INH05	-0.201	0.262	0.252	-2.805
INH06	-0.407	0.221	0.22	-2.859
INH07	-0.097	0.214	-0.38	-2.947
INH08	-0.015	0.17	-0.404	-2.946

INH09	0.114	0.098	0.053	-2.216
INH10	-0.329	0.071	-0.854	-2.742
INH11	-0.322	0.227	-0.479	-2.986
INH12	-0.277	0.118	-0.553	-2.491
INH13	-0.612	0.45	-0.3	-2.881
INH14	0.212	0.031	0.271	-2.108
INH15	-0.049	0.201	0.34	-2.254
INH16	-0.298	0.293	0.261	-2.836
INH17	-0.431	0.089	-0.574	-2.472
INH18	-0.012	0.107	0.317	-2.246
INH19	0.081	0.067	0.208	-1.973
INH	-0.432	0.728	-0.117	-3.022

**Table 6B:** Distribution Properties of the Predicted Compounds.

**Abbreviations:** Distribution Volume in Humans (VD<sub>ss</sub>, Log L/kg), Fraction Unbound (FU), Blood blood-brain barrier Permeability (LogBB), and Central Nervous System Permeability (LogPS). Gray shading indicates low values, green represents moderate values, and Tuscan signifies high values.

Codes	CYP 1A2	CYP 3A4		CYP 2C9	CYP 2C19	CYP 2D6	
	Inhi	Inhi	Subs	inhi	Inhi	Inhi	Subs
NH01	Yes	No	Yes	No	No	No	No
NH02	Yes	No	No	No	No	No	No
NH03	Yes	No	Yes	No	No	No	No
NH04	Yes	No	Yes	No	Yes	No	No
NH05	Yes	No	No	No	No	No	No
NH06	No	No	Yes	No	No	No	No
NH07	Yes	No	Yes	No	No	No	No
NH08	Yes	No	Yes	No	No	No	No
NH09	Yes	No	Yes	No	Yes	No	No
NH10	Yes	No	Yes	No	Yes	No	No
NH11	Yes	No	No	No	No	No	No
NH12	Yes	No	Yes	No	No	No	No
NH13	Yes	No	No	No	No	No	No
NH14	Yes	No	Yes	Yes	Yes	No	No
NH15	Yes	No	Yes	No	No	No	No

NH16	Yes	No	No	No	No	No	No
NH17	Yes	No	Yes	No	No	No	No
NH18	Yes	Yes	Yes	No	Yes	No	No
NH19	Yes	No	Yes	No	Yes	No	No
NH	No	No	No	No	No	No	No

**Table 6C:** Metabolism Properties of the Predicted Compounds.

**Abbreviations:** CYP (Cytochrome P450), Inhi (Inhibitor), Subs (Substrate). The pink color and "Yes" indicate an effect on the target, while the white color and "No" indicate no effect on the target.

Codes	Excretion	
	CL <sub>tot</sub> Log ml/min/kg	Renal OCT2 substrate (Yes/ No)
INH01	0.717	No
INH02	0.665	No
INH03	0.744	No
INH04	-0.054	No
INH05	0.873	No
INH06	0.822	No
INH07	0.771	No
INH08	0.821	No
INH09	0.684	No
INH10	0.834	No
INH11	0.841	No
INH12	0.712	No
INH13	0.757	No
INH14	0.966	No
INH15	0.759	No
INH16	0.027	No
INH17	0.691	No
INH18	0.834	No
INH19	0.678	No
INH	0.782	No

**Table 6D:** Excretion Properties of the Predicted Compounds.

### Abbreviations

Total clearance (CL<sub>tot</sub>), Organic cation transporter 2 (OCT2). The gray color represents low, the green color represents moderate, and the

Tuscan color represents high clearance in accordance with the value by Log ml/min/kg.

## References

- Aboui-Fadl, T., Abdei, F., Mohammed, H., Abdei, E., & Hassan, -Saboor. (2003). Synthesis, Antitubercular Activity and Pharmacokinetic Studies of Some Schiff Bases Derived from 1-Alkylisatin and Isonicotinic Acid Hydrazide (INH). In *Arch Pharm Res* (Vol. 26, Issue 10). <http://apr.psk.or.kr>
- Abraham, M. H., Chadha, H. S., & Mitchell, R. C. (1993). Hydrogen Bonding. 33. Factors That Influence the Distribution of Solutes between Blood and Brain.
- Ahmad, S., Qazi, S., & Raza, K. (2021). Translational bioinformatics methods for drug discovery and drug repurposing. In *Translational Bioinformatics in Healthcare and Medicine* (Vol. 13, pp. 127–139). Elsevier Science Ltd. <https://doi.org/10.1016/B978-0-323-89824-9.00010-0>
- Alex, A., Millan, D. S., Perez, M., Wakenhut, F., & Whitlock, G. A. (2011). Intramolecular hydrogen bonding to improve membrane permeability and absorption in beyond rule of five chemical space. *MedChemComm*, 2(7), 669–674. <https://doi.org/10.1039/c1md00093d>
- Azman, M., Sabri, A. H., Anjani, Q. K., Mustaffa, M. F., & Hamid, K. A. (2022). Intestinal Absorption Study: Challenges and Absorption Enhancement Strategies in Improving Oral Drug Delivery. In *Pharmaceuticals* (Vol. 15, Issue 8). MDPI. <https://doi.org/10.3390/ph15080975>
- Balamurugan, R., Stalin, A., & Ignacimuthu, S. (2012). Molecular docking of  $\gamma$ -sitosterol with some targets related to diabetes. *European Journal of Medicinal Chemistry*, 47(1), 38–43. <https://doi.org/10.1016/j.ejmech.2011.10.007>
- Barrett, J. A., Yang, W., Skolnik, S. M., Belliveau, L. M., & Patros, K. M. (2022). Discovery solubility measurement and assessment of small molecules with drug development in mind. In *Drug Discovery Today* (Vol. 27, Issue 5, pp. 1315–1325). Elsevier Ltd. <https://doi.org/10.1016/j.drudis.2022.01.017>
- Benedetti, F. (2014). Drugs and placebos: What's the difference?: Understanding the molecular basis of the placebo effect could help clinicians to better use it in clinical practice. *EMBO Reports*, 15(4), 329–332. <https://doi.org/10.1002/embr.201338399>
- Berellini, G., Springer, C., Waters, N. J., & Lombardo, F. (2009). In silico prediction of volume of distribution in human using linear and nonlinear models on a 669 compound data set. *Journal of Medicinal Chemistry*, 52(14), 4488–4495. <https://doi.org/10.1021/jm9004658>
- Bicker, J., Alves, G., Falcão, A., & Fortuna, A. (2020). Timing in drug absorption and disposition: The past, present, and future of chronopharmacokinetics. In *British Journal of Pharmacology* (Vol. 177, Issue 10, pp. 2215–2239). John Wiley and Sons Inc. <https://doi.org/10.1111/bph.15017>
- Burckhardt, G., & Wolff, N. A. (2000). invited review Structure of renal organic anion and cation transporters. <http://www.ajprenal.org>
- Calixto, A. R., Ramos, M. J., & Fernandes, P. A. (2019). Conformational diversity induces nanosecond-timescale chemical disorder in the HIV-1 protease reaction pathway. *Chemical Science*, 10(30), 7212–7221. <https://doi.org/10.1039/c9sc01464k>
- Cha, Y., Erez, T., Reynolds, I. J., Kumar, D., Ross, J., Koytiger, G., Kusko, R., Zeskind, B., Risso, S., Kagan, E., Papapetropoulos, S., Grossman, I., & Laifenfeld, D. (2018). Drug repurposing from the perspective of pharmaceutical companies. In *British Journal of Pharmacology* (Vol. 175, Issue 2, pp. 168–180). John Wiley and Sons Inc. <https://doi.org/10.1111/bph.13798>
- Chander, S., Tang, C. R., Al-Maqtari, H. M., Jamalis, J., Penta, A., Hadda, T. Ben, Sirat, H. M., Zheng, Y. T. et al. (2017). Synthesis and study of anti-HIV-1 RT activity of 5-benzoyl-4-methyl-1,3,4,5-tetrahydro-2H-1,5-benzodiazepin-2-one derivatives. *Bioorganic Chemistry*, 72, 74–79. <https://doi.org/10.1016/j.bioorg.2017.03.013>
- Chen, Z., Li, Y., Chen, E., Hall, D. L., Darke, P. L. et al. (1994). Crystal Structure at 1.9-Å Resolution of Human Immunodeficiency Virus (HIV) II Protease Complexed with L-735,524, an Orally Bioavailable Inhibitor of the HIV Proteases. *Journal of Biological Chemistry*, 269(42), 26344–26348. [https://doi.org/10.1016/s0021-9258\(18\)47199-2](https://doi.org/10.1016/s0021-9258(18)47199-2)
- Chua, H. M., Moshawih, S., Goh, H. P., Ming, L. C., & Kifli, N. (2023). Insights into the computer-aided drug design and discovery based on anthraquinone scaffold for cancer treatment: A protocol for systematic review. *PLoS ONE*, 18(9 September). <https://doi.org/10.1371/journal.pone.0290948>
- Clark, D. E. (2011). What has polar surface area ever done for drug discovery? In *Future Medicinal Chemistry* (Vol. 3, Issue 4, pp. 469–484). <https://doi.org/10.4155/fmc.11.1>
- Cordery, S. F., Pensado, A., Chiu, W. S., Shehab, M. Z., Bunge, A. L. et al. (2017). Topical bioavailability of diclofenac from locally-acting, dermatological formulations. *International Journal of Pharmaceutics*, 529(1–2), 55–64. <https://doi.org/10.1016/j.ijpharm.2017.06.063>
- Côrte-Real, L., Karas, B., Gírio, P., Moreno, A., Avecilla, F. et al. (2019). Unprecedented inhibition of P-gp activity by a novel ruthenium-cyclopentadienyl compound bearing a bipyridine-biotin ligand. *European Journal of Medicinal Chemistry*, 163, 853–863. <https://doi.org/10.1016/j.ejmech.2018.12.022>
- Crivori, P., Cruciani, G., Carrupt, P.-A., & Testa, B. (2000). Predicting Blood-Brain Barrier Permeation from Three-Dimensional Molecular Structure. <https://doi.org/10.1021/jm990968>
- Currie, G. M. (2018a). Pharmacology, part 1: Introduction to pharmacology and pharmacodynamics. *Journal of Nuclear Medicine Technology*, 46(2), 81–86. <https://doi.org/10.2967/jnmt.117.199588>
- Currie, G. M. (2018b). Pharmacology, part 2: Introduction to pharmacokinetics. *Journal of Nuclear Medicine Technology*, 46(3), 221–230. <https://doi.org/10.2967/jnmt.117.199638>
- de Souza Neto, L. R., Moreira-Filho, J. T., Neves, B. J., Maidana, R. L. B. R., Guimarães, A. C. R. et al. (2020). In silico Strategies to Support Fragment-to-Lead Optimization in Drug Discovery. In *Frontiers in Chemistry* (Vol. 8). Frontiers Media S.A. <https://doi.org/10.3389/fchem.2020.00093>
- Decherchi, S., & Cavalli, A. (2020). Thermodynamics and Kinetics of Drug-Target Binding by Molecular Simulation. In *Chemical Reviews* (Vol. 120, Issue 23, pp. 12788–12833). American Chemical Society. <https://doi.org/10.1021/acs.chemrev.0c00534>
- Delaney, J. S. (2004). ESOL: Estimating aqueous solubility directly from molecular structure. *Journal of Chemical Information and Computer Sciences*, 44(3), 1000–1005. <https://doi.org/10.1021/ci034243x>
- Dong, J., Qin, Z., Zhang, W. D., Cheng, G., Yehuda, A. G. et al. (2020). Medicinal chemistry strategies to discover P-glycoprotein inhibitors: An update. In *Drug Resistance Updates* (Vol. 49). Churchill Livingstone. <https://doi.org/10.1016/j.drug.2020.100681>
- Doyon, L., Tremblay, S., Bourgon, L., Wardrop, E., & Cordingley, M. G. (2005). Selection and characterization of HIV-1 showing reduced susceptibility to the non-peptidic protease inhibitor tipranavir. *Antiviral Research*, 68(1), 27–35. <https://doi.org/10.1016/j.antiviral.2005.07.003>
- Duan, H., Liu, X., Zhuo, W., Meng, J., Gu, J. et al. (2019). 3D-QSAR and molecular recognition of Klebsiella pneumoniae

- NDM-1 inhibitors. *Molecular Simulation*, 45(9), 694–705. <https://doi.org/10.1080/08927022.2019.1579327>
29. Elmeliegy, M., Vourvahis, M., Guo, C., & Wang, D. D. (2020). Effect of P-glycoprotein (P-gp) Inducers on Exposure of P-gp Substrates: Review of Clinical Drug–Drug Interaction Studies. In *Clinical Pharmacokinetics* (Vol. 59, Issue 6, pp. 699–714). Adis. <https://doi.org/10.1007/s40262-020-00867-1>
  30. Ertl, P., Rohde, B., & Selzer, P. (2000). Fast calculation of molecular polar surface area as a sum of fragment-based contributions and its application to the prediction of drug transport properties. *Journal of Medicinal Chemistry*, 43(20), 3714–3717. <https://doi.org/10.1021/jm000942e>
  31. Feher, M., Sourial, E., & Schmidt, J. M. (2000). A simple model for the prediction of blood-brain partitioning. In *International Journal of Pharmaceutics* (Vol. 201). [www.elsevier.com/locate/ijpharm](http://www.elsevier.com/locate/ijpharm)
  32. Filimonov, D. A., Lagunin, A. A., Glorizova, T. A., Rudik, A. V., Druzhilovskii, D. S. et al. (2014). PREDICTION OF THE BIOLOGICAL ACTIVITY SPECTRA OF ORGANIC COMPOUNDS USING THE PASS ONLINE WEB RESOURCE. In *Chemistry of Heterocyclic Compounds* (Vol. 50, Issue 3). <http://www.way2drug.com/passonline>
  33. Firmino, G. S. S., de Souza, M. V. N., Pessoa, C., Lourenco, M. C. S., Resende, J. A. L. C. et al. (2016). Synthesis and evaluation of copper(II) complexes with isoniazid-derived hydrazones as anticancer and antitubercular agents. *BioMetals*, 29(6), 953–963. <https://doi.org/10.1007/s10534-016-9968-7>
  34. Flatow, D., Leelananda, S. P., Skliros, A., Kloczkowski, A., & Jernigan, R. L. (2014). Send Orders for Reprints to [reprints@benthamscience.net](mailto:reprints@benthamscience.net) Volumes and Surface Areas: Geometries and Scaling Relationships between Coarse-Grained and Atomic Structures. In *Current Pharmaceutical Design* (Vol. 20).
  35. Fromm, M. F. (2004). Importance of P-glycoprotein at blood-tissue barriers. In *Trends in Pharmacological Sciences* (Vol. 25, Issue 8, pp. 423–429). <https://doi.org/10.1016/j.tips.2004.06.002>
  36. García-Sosa, A. T., Maran, U., & Hetényi, C. (2012). Molecular Property Filters Describing Pharmacokinetics and Drug Binding. In *Current Medicinal Chemistry* (Vol. 19).
  37. Gazerani, P. (2019). Identification of novel analgesics through a drug repurposing strategy. In *Pain Management* (Vol. 9, Issue 4, pp. 399–415). Newlands Press Ltd. <https://doi.org/10.2217/pmt-2018-0091>
  38. Gleeson, M. P., Hersey, A., Montanari, D., & Overington, J. (2011). Probing the links between in vitro potency, ADMET and physicochemical parameters. *Nature Reviews Drug Discovery*, 10(3), 197–208. <https://doi.org/10.1038/nrd3367>
  39. Habala, L., Varényi, S., Bilková, A., Herich, P., Valentová, J., Kožíšek, J., & Devinsky, F. (2016). Antimicrobial activity and urease inhibition of Schiff bases derived from isoniazid and fluorinated benzaldehydes and of their copper(II) complexes. *Molecules*, 21(12). <https://doi.org/10.3390/molecules21121742>
  40. Hsu, F., Chen, Y. C., & Broccatelli, F. (2021). Evaluation of tissue binding in three tissues across five species and prediction of volume of distribution from plasma protein and tissue binding with an existing model. *Drug Metabolism and Disposition*, 49(4), 330–336. <https://doi.org/10.1124/dmd.120.000337>
  41. Jackson, N., Czaplewski, L., & Piddock, L. J. V. (2018). Discovery and development of new antibacterial drugs: Learning from experience? In *Journal of Antimicrobial Chemotherapy* (Vol. 73, Issue 6, pp. 1452–1459). Oxford University Press. <https://doi.org/10.1093/jac/dky019>
  42. Kapetanovic, I. M. (2008). Computer-aided drug discovery and development (CADD): In silico-chemico-biological approach. *Chemico-Biological Interactions*, 171(2), 165–176. <https://doi.org/10.1016/j.cbi.2006.12.006>
  43. Khan, G., Sheek-Hussein, M., Al Suwaidi, A., Idris, K., & Abu-Zidan, F. (2020). Novel coronavirus pandemic: A global health threat. In *Turkish Journal of Emergency Medicine* (Vol. 20, Issue 2, pp. 55–62). Wolters Kluwer Medknow Publications. <https://doi.org/10.4103/2452-2473.285016>
  44. Khan, T., Dixit, S., Ahmad, R., Raza, S., Azad, I., Joshi, S., & Khan, A. R. (2017). Molecular docking, PASS analysis, bioactivity score prediction, synthesis, characterization and biological activity evaluation of a functionalized 2-butanone thiosemicarbazone ligand and its complexes. *Journal of Chemical Biology*, 10(3), 91–104. <https://doi.org/10.1007/s12154-017-0167-y>
  45. Khanna, V., & Ranganathan, S. (2009). Physicochemical property space distribution among human metabolites, drugs and toxins. *BMC Bioinformatics*, 10(SUPPL. 15). <https://doi.org/10.1186/1471-2105-10-S15-S10>
  46. Komura, H., Watanabe, R., & Mizuguchi, K. (2023). The Trends and Future Prospective of In Silico Models from the Viewpoint of ADME Evaluation in Drug Discovery. In *Pharmaceutics* (Vol. 15, Issue 11). Multidisciplinary Digital Publishing Institute (MDPI). <https://doi.org/10.3390/pharmaceutics15112619>
  47. König, J., Müller, F., & Fromm, M. F. (2013). Transporters and drug-drug interactions: Important determinants of drug disposition and effects. In *Pharmacological Reviews* (Vol. 65, Issue 3, pp. 944–966). <https://doi.org/10.1124/pr.113.007518>
  48. Kroschinsky, F., Stölzel, F., von Bonin, S., Beutel, G., Kochanek, M. et al. (2017). New drugs, new toxicities: Severe side effects of modern targeted and immunotherapy of cancer and their management. In *Critical Care* (Vol. 21, Issue 1). BioMed Central Ltd. <https://doi.org/10.1186/s13054-017-1678-1>
  49. Kumari, S., Singh, K., & Mukopadaya, S. (2022). review on the modern drug discovery process. *International Journal of Health Sciences*, 2043–2048. <https://doi.org/10.53730/ijhs.v6ns6.10207>
  50. Kus, M., Ibragimow, I., & Piotrowska-Kempisty, H. (2023). Caco-2 Cell Line Standardization with Pharmaceutical Requirements and In Vitro Model Suitability for Permeability Assays. In *Pharmaceutics* (Vol. 15, Issue 11). Multidisciplinary Digital Publishing Institute (MDPI). <https://doi.org/10.3390/pharmaceutics15112523>
  51. Lagorce, D., Douguet, D., Miteva, M. A., & Villoutreix, B. O. (2017). Computational analysis of calculated physicochemical and ADMET properties of protein-protein interaction inhibitors. *Scientific Reports*, 7. <https://doi.org/10.1038/srep46277>
  52. La-Scalea, M. A., Souza Menezes, C. M., & Ferreira, E. I. (2005). Molecular volume calculation using AM1 semi-empirical method toward diffusion coefficients and electrophoretic mobility estimates in aqueous solution. *Journal of Molecular Structure: THEOCHEM*, 730(1–3), 111–120. <https://doi.org/10.1016/j.theochem.2005.05.030>
  53. Lee, K., Jang, J., Seo, S., Lim, J., & Kim, W. Y. (2022a). Drug-likeness scoring based on unsupervised learning. *Chemical Science*, 13(2), 554–565. <https://doi.org/10.1039/d1sc05248a>
  54. Lee, K., Jang, J., Seo, S., Lim, J., & Kim, W. Y. (2022b). Drug-likeness scoring based on unsupervised learning. *Chemical Science*, 13(2), 554–565. <https://doi.org/10.1039/d1sc05248a>
  55. Leeson, P. D. (2016). Molecular inflation, attrition and the rule of five. In *Advanced Drug Delivery Reviews* (Vol. 101, pp.

- 22–33). Elsevier B.V. <https://doi.org/10.1016/j.addr.2016.01.018>
56. Leeson, P. D., & Young, R. J. (2015). Molecular Property Design: Does Everyone Get It? *ACS Medicinal Chemistry Letters*, 6(7), 722–725. <https://doi.org/10.1021/acsmchemlett.5b00157>
  57. Liao, J., Wang, Q., Wu, F., & Huang, Z. (2022). In Silico Methods for Identification of Potential Active Sites of Therapeutic Targets. In *Molecules* (Vol. 27, Issue 20). MDPI. <https://doi.org/10.3390/molecules27207103>
  58. Lienx, E. J., & Wang, P. H. (1980). Lipophilicity, Molecular Weight, and Drug Action: Reexamination of Parabolic and Bilinear Models. In *Journal of Pharmaceutical Sciences* (Vol. 69, Issue 6).
  59. Lin, K., Kong, X., Tao, X., Zhai, X., Lv, L. et al. (2023). Research Methods and New Advances in Drug–Drug Interactions Mediated by Renal Transporters. In *Molecules* (Vol. 28, Issue 13). Multidisciplinary Digital Publishing Institute (MDPI). <https://doi.org/10.3390/molecules28135252>
  60. Ling, Y., Hao, Z. Y., Liang, D., Zhang, C. L., Liu, Y. F. et al. (2021). The expanding role of pyridine and dihydropyridine scaffolds in drug design. In *Drug Design, Development and Therapy* (Vol. 15, pp. 4289–4338). Dove Medical Press Ltd. <https://doi.org/10.2147/DDDT.S329547>
  61. Lipinski, C. A. (2004). Lead- and drug-like compounds: The rule-of-five revolution. In *Drug Discovery Today: Technologies* (Vol. 1, Issue 4, pp. 337–341). <https://doi.org/10.1016/j.ddtec.2004.11.007>
  62. Lipinski, C. A., Lombardo, F., Dominy, B. W., & Feeney, P. J. (2001). Experimental and computational approaches to estimate solubility and permeability in drug discovery and development settings. In *Advanced Drug Delivery Reviews* (Vol. 46). [www.elsevier.com/locate/drugdeliv](http://www.elsevier.com/locate/drugdeliv)
  63. Lucas, A. J., Sproston, J. L., Barton, P., & Riley, R. J. (2019). Estimating human ADME properties, pharmacokinetic parameters and likely clinical dose in drug discovery. In *Expert Opinion on Drug Discovery* (Vol. 14, Issue 12, pp. 1313–1327). Taylor and Francis Ltd. <https://doi.org/10.1080/17460441.2019.1660642>
  64. Mali, S. N., Thorat, B. R., Gupta, D. R., & Pandey, A. (2021). Mini-Review of the Importance of Hydrazides and Their Derivatives—Synthesis and Biological Activity †. *Engineering Proceedings*, 11(1). <https://doi.org/10.3390/ASEC2021-11157>
  65. McGowan, J. C. (1956). MOLECULAR VOLUMES AND STRUCTURAL CHEMISTRY.
  66. Meanwell, N. A. (2011). Improving drug candidates by design: A focus on physicochemical properties as a means of improving compound disposition and safety. In *Chemical Research in Toxicology* (Vol. 24, Issue 9, pp. 1420–1456). <https://doi.org/10.1021/tx200211v>
  67. Morozov, A. V., & Kortemme, T. (2005). Potential Functions for Hydrogen Bonds in Protein Structure Prediction and Design. In *Advances in Protein Chemistry* (Vol. 72, pp. 1–38). [https://doi.org/10.1016/S0065-3233\(05\)72001-5](https://doi.org/10.1016/S0065-3233(05)72001-5)
  68. Motl, S., Zhuang, Y., Waters, C. M., & Stewart, C. F. (2006). Pharmacokinetic Considerations in the Treatment of CNS Tumours. In *Clin Pharmacokinetics* (Vol. 45, Issue 9).
  69. Mushtaque, M., & Rizvi, M. M. A. (2023). Molecular hybrids based on Pyrazole and 4-Thiazolidinone cores: Synthesis, characterization, and anticancer studies. *Journal of Molecular Structure*, 1294. <https://doi.org/10.1016/j.molstruc.2023.136470>
  70. Neves, R. P. P., Fernandes, P. A., & Ramos, M. J. (2017). Mechanistic insights on the reduction of glutathione disulfide by protein disulfide isomerase. *Proceedings of the National Academy of Sciences of the United States of America*, 114(24), E4724–E4733. <https://doi.org/10.1073/pnas.1618985114>
  71. Nielsen, R. B., Larsen, B. S., Holm, R., Pijpers, I., Snoeys, J., Nielsen, U. G. et al. (2023). Increased bioavailability of a P-gp substrate: Co-release of etoposide and zosuquidar from amorphous solid dispersions. *International Journal of Pharmaceutics*, 642. <https://doi.org/10.1016/j.ijpharm.2023.123094>
  72. Njogu, P. M., Guantai, E. M., Pavada, E., & Chibale, K. (2016). Computer-Aided Drug Discovery Approaches against the Tropical Infectious Diseases Malaria, Tuberculosis, Trypanosomiasis, and Leishmaniasis. In *ACS Infectious Diseases* (Vol. 2, Issue 1, pp. 8–31). *American Chemical Society*. <https://doi.org/10.1021/acsinfectdis.5b00093>
  73. Pace, C. N., Fu, H., Fryar, K. L., Landua, J., Trevino, S. R. et al. (2011). Contribution of hydrophobic interactions to protein stability. *Journal of Molecular Biology*, 408(3), 514–528. <https://doi.org/10.1016/j.jmb.2011.02.053>
  74. Parasuraman, S. (2011). Prediction of activity spectra for substances. In *Journal of Pharmacology and Pharmacotherapeutics* (Vol. 2, Issue 1, pp. 52–53). <https://doi.org/10.4103/0976-500X.77119>
  75. Pardridge, W. M. (2012). Drug transport across the blood-brain barrier. In *Journal of Cerebral Blood Flow and Metabolism* (Vol. 32, Issue 11, pp. 1959–1972). <https://doi.org/10.1038/jcbfm.2012.126>
  76. Pennington, L. D., & Moustakas, D. T. (2017). The Necessary Nitrogen Atom: A Versatile High-Impact Design Element for Multiparameter Optimization. In *Journal of Medicinal Chemistry* (Vol. 60, Issue 9, pp. 3552–3579). *American Chemical Society*. <https://doi.org/10.1021/acs.jmedchem.6b01807>
  77. Pensado, A., McGrogan, A., White, K. A. J., Bunge, A. L., Guy, R. H. et al. (2022). Assessment of dermal bioavailability: predicting the input function for topical glucocorticoids using stratum corneum sampling. *Drug Delivery and Translational Research*, 12(4), 851–861. <https://doi.org/10.1007/s13346-021-01064-8>
  78. Pires, D. E. V., Blundell, T. L., & Ascher, D. B. (2015). pkCSM: Predicting small-molecule pharmacokinetic and toxicity properties using graph-based signatures. *Journal of Medicinal Chemistry*, 58(9), 4066–4072. <https://doi.org/10.1021/acs.jmedchem.5b00104>
  79. Pollock, J. R., Anderson, S. T., Elahi, M. A., & Moore, M. L. (2024). Drug discovery. In *Translational Orthopedics* (pp. 33–38). Elsevier. <https://doi.org/10.1016/B978-0-323-85663-8.00027-1>
  80. Pushpakom, S., Iorio, F., Eyers, P. A., Escott, K. J., Hopper, S., Wells, A., Doig, A., Guillems, T., Latimer, J., McNamee, C., Norris, A., Sanseau, P., Cavalla, D., & Pirmohamed, M. (2018). Drug repurposing: Progress, challenges and recommendations. In *Nature Reviews Drug Discovery* (Vol. 18, Issue 1, pp. 41–58). Nature Publishing Group. <https://doi.org/10.1038/nrd.2018.168>
  81. Raczuk, E., Dmochowska, B., Samaszko-Fiertek, J., & Madaj, J. (2022). Different Schiff Bases—Structure, Importance and Classification. In *Molecules* (Vol. 27, Issue 3). MDPI. <https://doi.org/10.3390/molecules27030787>
  82. Reddy, R. N., Mutyala, R., Aparoy, P., Reddanna, P., & Reddy, M. R. (2007). Computer Aided Drug Design Approaches to Develop Cyclooxygenase Based Novel Anti-Inflammatory and Anti-Cancer Drugs. In *Current Pharmaceutical Design* (Vol. 13).
  83. Rezai, T., Bock, J. E., Zhou, M. V., Kalyanaraman, C., Lokey, R. S., & Jacobson, M. P. (2006). Conformational flexibility,

- internal hydrogen bonding, and passive membrane permeability: Successful in silico prediction of the relative permeabilities of cyclic peptides. *Journal of the American Chemical Society*, 128(43), 14073–14080. <https://doi.org/10.1021/ja063076p>
84. Rodrigues, F. A. R., Oliveira, A. C. A., Cavalcanti, B. C., Pessoa, C., Pinheiro, A. C., & De Souza, M. V. N. (2014). Biological evaluation of isoniazid derivatives as an anticancer class. *Scientia Pharmaceutica*, 82(1), 21–28. <https://doi.org/10.3797/scipharm.1307-25>
  85. Rohilla, S., Goyal, G., Berwal, P., & Mathur, N. (2024). A Review on Indole-triazole Molecular Hybrids as a Leading Edge in Drug Discovery: Current Landscape and Future Perspectives. *Current Topics in Medicinal Chemistry*, 24(18), 1557–1588. <https://doi.org/10.2174/0115680266307132240509065351>
  86. Roman, R., Pintilie, L., Nuță, D., Avram, S., Buiu, C. et al. (2023). In Silico Prediction, Characterization and Molecular Docking Studies on New Benzamide Derivatives. *Processes*, 11(2). <https://doi.org/10.3390/pr11020479>
  87. Ruiz-Garcia, A., Bermejo, M., Moss, A., & Casabo, V. G. (2008). Pharmacokinetics in drug discovery. In *Journal of Pharmaceutical Sciences* (Vol. 97, Issue 2, pp. 654–690). John Wiley and Sons Inc. <https://doi.org/10.1002/jps.21009>
  88. Saaby, L., & Brodin, B. (2017). A Critical View on In Vitro Analysis of P-glycoprotein (P-gp) Transport Kinetics. In *Journal of Pharmaceutical Sciences* (Vol. 106, Issue 9, pp. 2257–2264). Elsevier B.V. <https://doi.org/10.1016/j.xphs.2017.04.022>
  89. Sachin S Padole, Alpna J Asnani, Dinesh R Chaple, & Soumya G Katre. (2022). A review of approaches in computer-aided drug design in drug discovery. *GSC Biological and Pharmaceutical Sciences*, 19(2), 075–083. <https://doi.org/10.30574/gscbps.2022.19.2.0161>
  90. Salazar, D. E., & Gormley, G. (2017). Modern Drug Discovery and Development. In *Clinical and Translational Science: Principles of Human Research: Second Edition* (pp. 719–743). Elsevier Inc. <https://doi.org/10.1016/B978-0-12-802101-9.00041-7>
  91. Sampat, G., Suryawanshi, S. S., Palled, M. S., Patil, A. S., Khanal, P. et al. (2022). Drug Likeness Screening and Evaluation of Physicochemical Properties of Selected Medicinal Agents by Computer Aided Drug Design Tools. *Advances in Pharmacology and Pharmacy*, 10(4), 234–246. <https://doi.org/10.13189/app.2022.100402>
  92. Santos, D. C., Henriques, R. R., Junior, M. A. de A. L., Farias, A. B. et al. (2020). Acylhydrazones as isoniazid derivatives with multi-target profiles for the treatment of Alzheimer's disease: Radical scavenging, myeloperoxidase/acetylcholinesterase inhibition and biometal chelation. *Bioorganic and Medicinal Chemistry*, 28(10). <https://doi.org/10.1016/j.bmc.2020.115470>
  93. Santos-Martins, D., & Forli, S. (2020). Charting Hydrogen Bond Anisotropy. *Journal of Chemical Theory and Computation*, 16(4), 2846–2856. <https://doi.org/10.1021/acs.jctc.9b01248>
  94. Schlander, M., Hernandez-Villafuerte, K., Cheng, C. Y., Mestre-Ferrandiz, J., & Baumann, M. (2021). How Much Does It Cost to Research and Develop a New Drug? A Systematic Review and Assessment. In *PharmacoEconomics* (Vol. 39, Issue 11, pp. 1243–1269). Adis. <https://doi.org/10.1007/s40273-021-01065-y>
  95. Semighini, E. P., Resende, J. A., De Andrade, P., Morais, P. A. B., Carvalho, I., Taft, C. A. et al. (2011). Using computer-aided drug design and medicinal chemistry strategies in the fight against diabetes. *Journal of Biomolecular Structure and Dynamics*, 28(5), 787–796. <https://doi.org/10.1080/07391102.2011.10508606>
  96. Seyfinejad, B., Ozkan, S. A., & Jouyban, A. (2021). Recent advances in the determination of unbound concentration and plasma protein binding of drugs: Analytical methods. In *Talanta* (Vol. 225). Elsevier B.V. <https://doi.org/10.1016/j.talanta.2020.122052>
  97. Shinoda, W. (2016). Permeability across lipid membranes. *Biochimica et Biophysica Acta - Biomembranes*, 1858(10), 2254–2265. <https://doi.org/10.1016/j.bbamem.2016.03.032>
  98. Sinha, S., & Vohora, D. (2017). Drug Discovery and Development: An Overview. In *Pharmaceutical Medicine and Translational Clinical Research* (pp. 19–32). Elsevier Inc. <https://doi.org/10.1016/B978-0-12-802103-3.00002-X>
  99. Sliwoski, G., Kothiwale, S., Meiler, J., & Lowe, E. W. (2014). Computational methods in drug discovery. In *Pharmacological Reviews* (Vol. 66, Issue 1, pp. 334–395). <https://doi.org/10.1124/pr.112.007336>
  100. Subbiah, V. (2023). The next generation of evidence-based medicine. *Nature Medicine*, 29(1), 49–58. <https://doi.org/10.1038/s41591-022-02160-z>
  101. Sun, D., Gao, W., Hu, H., & Zhou, S. (2022). Why 90% of clinical drug development fails and how to improve it? In *Acta Pharmaceutica Sinica B* (Vol. 12, Issue 7, pp. 3049–3062). Chinese Academy of Medical Sciences. <https://doi.org/10.1016/j.apsb.2022.02.002>
  102. Supuran, C. T. (2017). Advances in structure-based drug discovery of carbonic anhydrase inhibitors. In *Expert Opinion on Drug Discovery* (Vol. 12, Issue 1, pp. 61–88). Taylor and Francis Ltd. <https://doi.org/10.1080/17460441.2017.1253677>
  103. Talevi, A., & Bellera, C. L. (2018). Drug Excretion. In *ADME Processes in Pharmaceutical Sciences: Dosage, Design, and Pharmacotherapy Success* (pp. 81–96). Springer International Publishing. [https://doi.org/10.1007/978-3-319-99593-9\\_5](https://doi.org/10.1007/978-3-319-99593-9_5)
  104. Talevi, A., & Bellera, C. L. (2020a). Challenges and opportunities with drug repurposing: finding strategies to find alternative uses of therapeutics. In *Expert Opinion on Drug Discovery* (Vol. 15, Issue 4, pp. 397–401). Taylor and Francis Ltd. <https://doi.org/10.1080/17460441.2020.1704729>
  105. Talevi, A., & Bellera, C. L. (2020b). Challenges and opportunities with drug repurposing: finding strategies to find alternative uses of therapeutics. In *Expert Opinion on Drug Discovery* (Vol. 15, Issue 4, pp. 397–401). Taylor and Francis Ltd. <https://doi.org/10.1080/17460441.2020.1704729>
  106. Tian, S., Wang, J., Li, Y., Li, D., Xu, L., & Hou, T. (2015). The application of in silico drug-likeness predictions in pharmaceutical research. In *Advanced Drug Delivery Reviews* (Vol. 86, pp. 2–10). Elsevier B.V. <https://doi.org/10.1016/j.addr.2015.01.009>
  107. Tran, T. T. Van, Tayara, H., & Chong, K. T. (2023). Recent Studies of Artificial Intelligence on In Silico Drug Absorption. In *Journal of Chemical Information and Modeling* (Vol. 63, Issue 20, pp. 6198–6211). American Chemical Society. <https://doi.org/10.1021/acs.jcim.3c00960>
  108. Tripathi, R. K. P., & Ayyannan, S. R. (2018). Evaluation of 2-amino-6-nitrobenzothiazole derived hydrazones as acetylcholinesterase inhibitors: in vitro assays, molecular docking and theoretical ADMET prediction. *Medicinal Chemistry Research*, 27(3), 709–725. <https://doi.org/10.1007/s00044-017-2095-3>
  109. Tsakovska, I., Pajeva, I., Al Sharif, M., Alov, P., Fioravanzo, E. et al. (2017). Quantitative structure-skin permeability relationships. In *Toxicology* (Vol. 387, pp. 27–42). Elsevier Ireland Ltd. <https://doi.org/10.1016/j.tox.2017.06.008>
  110. Tshepelevitsh, S., Kadam, S. A., Darnell, A., Bobacka, J., Rützel, A. et al. (2020). LogP determination for highly

- lipophilic hydrogen-bonding anion receptor molecules. *Analytica Chimica Acta*, 1132, 123–133. <https://doi.org/10.1016/j.aca.2020.07.024>
111. Uddin, N., Rashid, F., Ali, S., Tirmizi, S. A., Ahmad, I. et al. (2020). Synthesis, characterization, and anticancer activity of Schiff bases. *Journal of Biomolecular Structure and Dynamics*, 38(11), 3246–3259. <https://doi.org/10.1080/07391102.2019.1654924>
  112. van de Waterbeemd, H., & Gifford, E. (2003). ADMET in silico modelling: Towards prediction paradise? In *Nature Reviews Drug Discovery* (Vol. 2, Issue 3, pp. 192–204). <https://doi.org/10.1038/nrd1032>
  113. Veber, D. F., Johnson, S. R., Cheng, H. Y., Smith, B. R., Ward, K. W. et al. (2002). Molecular properties that influence the oral bioavailability of drug candidates. *Journal of Medicinal Chemistry*, 45(12), 2615–2623. <https://doi.org/10.1021/jm020017n>
  114. Vieth, M., Siegel, M. G., Higgs, R. E., Watson, I. A., Robertson, D. H. et al. (2004). Characteristic Physical Properties and Structural Fragments of Marketed Oral Drugs. *Journal of Medicinal Chemistry*, 47(1), 224–232. <https://doi.org/10.1021/jm030267j>
  115. Vilchèze, C., & Jacobs, W. R. (2019). The Isoniazid Paradigm of Killing, Resistance, and Persistence in Mycobacterium tuberculosis. In *Journal of Molecular Biology* (Vol. 431, Issue 18, pp. 3450–3461). Academic Press. <https://doi.org/10.1016/j.jmb.2019.02.016>
  116. Waghay, D., & Zhang, Q. (2018). Inhibit or Evade Multidrug Resistance P-Glycoprotein in Cancer Treatment. In *Journal of Medicinal Chemistry* (Vol. 61, Issue 12, pp. 5108–5121). American Chemical Society. <https://doi.org/10.1021/acs.jmedchem.7b01457>
  117. Wang, S., Dong, G., & Sheng, C. (2019). Structural simplification: an efficient strategy in lead optimization. In *Acta Pharmaceutica Sinica B* (Vol. 9, Issue 5, pp. 880–901). *Chinese Academy of Medical Sciences*. <https://doi.org/10.1016/j.apsb.2019.05.004>
  118. Waring, M. J. (2010). Lipophilicity in drug discovery. In *Expert Opinion on Drug Discovery* (Vol. 5, Issue 3, pp. 235–248). <https://doi.org/10.1517/17460441003605098>
  119. Watanabe, R., Esaki, T., Kawashima, H., Natsume-Kitatani, Y., Nagao, C. et al. (2018). Predicting Fraction Unbound in Human Plasma from Chemical Structure: Improved Accuracy in the Low Value Ranges. *Molecular Pharmaceutics*, 15(11), 5302–5311. <https://doi.org/10.1021/acs.molpharmaceut.8b00785>
  120. Wei, Y., Palazzolo, L., Ben Mariem, O., Bianchi, D., Laurenzi, T. et al. (2024). Investigation of in silico studies for cytochrome P450 isoforms specificity. In *Computational and Structural Biotechnology Journal* (Vol. 23, pp. 3090–3103). Elsevier B.V. <https://doi.org/10.1016/j.csbj.2024.08.002>
  121. Wright, S. H. (2019). Molecular and cellular physiology of organic cation transporter 2. *Am J Physiol Renal Physiol*, 317, 1669–1679. <https://doi.org/10.1152/ajprenal.00422.2019.-Organic>
  122. Wu, G., Zhao, T., Kang, D., Zhang, J., Song, Y. et al. (2019). Overview of Recent Strategic Advances in Medicinal Chemistry. In *Journal of Medicinal Chemistry* (Vol. 62, Issue 21, pp. 9375–9414). *American Chemical Society*. <https://doi.org/10.1021/acs.jmedchem.9b00359>
  123. Xiang, M., Cao, Y., Fan, W., Chen, L., & Mo, Y. (2012). Computer-Aided Drug Design: Lead Discovery and Optimization. In *Combinatorial Chemistry & High Throughput Screening* (Vol. 15). <http://predictioncenter.org/>
  124. Yang, W., Wang, Y., Han, D., Tang, W., & Sun, L. (2024). Recent advances in application of computer-aided drug design in anti-COVID-19 Virial Drug Discovery. In *Biomedicine and Pharmacotherapy* (Vol. 173). Elsevier Masson s.r.l. <https://doi.org/10.1016/j.biopha.2024.116423>
  125. Zanger, U. M., & Schwab, M. (2013). Cytochrome P450 enzymes in drug metabolism: Regulation of gene expression, enzyme activities, and impact of genetic variation. In *Pharmacology and Therapeutics* (Vol. 138, Issue 1, pp. 103–141). <https://doi.org/10.1016/j.pharmthera.2012.12.007>
  126. Zhang, Y., Wang, C., Jia, Z. li, Ma, R. jiao, Wang, X. et al. (2020). Isoniazid promotes the anti-inflammatory response in zebrafish associated with regulation of the PPAR $\gamma$ /NF- $\kappa$ B/AP-1 pathway. *Chemico-Biological Interactions*, 316. <https://doi.org/10.1016/j.cbi.2019.108928>



This work is licensed under Creative Commons Attribution 4.0 License

To Submit Your Article Click Here:

[Submit Manuscript](#)

DOI:10.31579/2690-1897/235

#### Ready to submit your research? Choose Auctores and benefit from:

- fast, convenient online submission
- rigorous peer review by experienced research in your field
- rapid publication on acceptance
- authors retain copyrights
- unique DOI for all articles
- immediate, unrestricted online access

At Auctores, research is always in progress.

Learn more <https://auctoresonline.org/journals/journal-of-surgical-case-reports-and-images>